

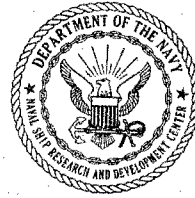
Ad 767021

GVTDOC
D 211.
9:
4095

Report 4095

SHIP RESEARCH AND DEVELOPMENT CENTER

Bethesda, Maryland 20034



SLAMMING TESTS OF THREE-DIMENSIONAL MODELS IN CALM WATER AND WAVES

LIBRARY

by

Sheng-Lun Chuang

SEP 22 1973

U. S. NAVAL ACADEMY

APPROVED FOR PUBLIC RELEASE: DISTRIBUTION UNLIMITED

20070122 070

STRUCTURES DEPARTMENT
RESEARCH AND DEVELOPMENT REPORT

LIBRARY

September 1973

DEC 5 1973

Report 4095

U. S. NAVAL ACADEMY

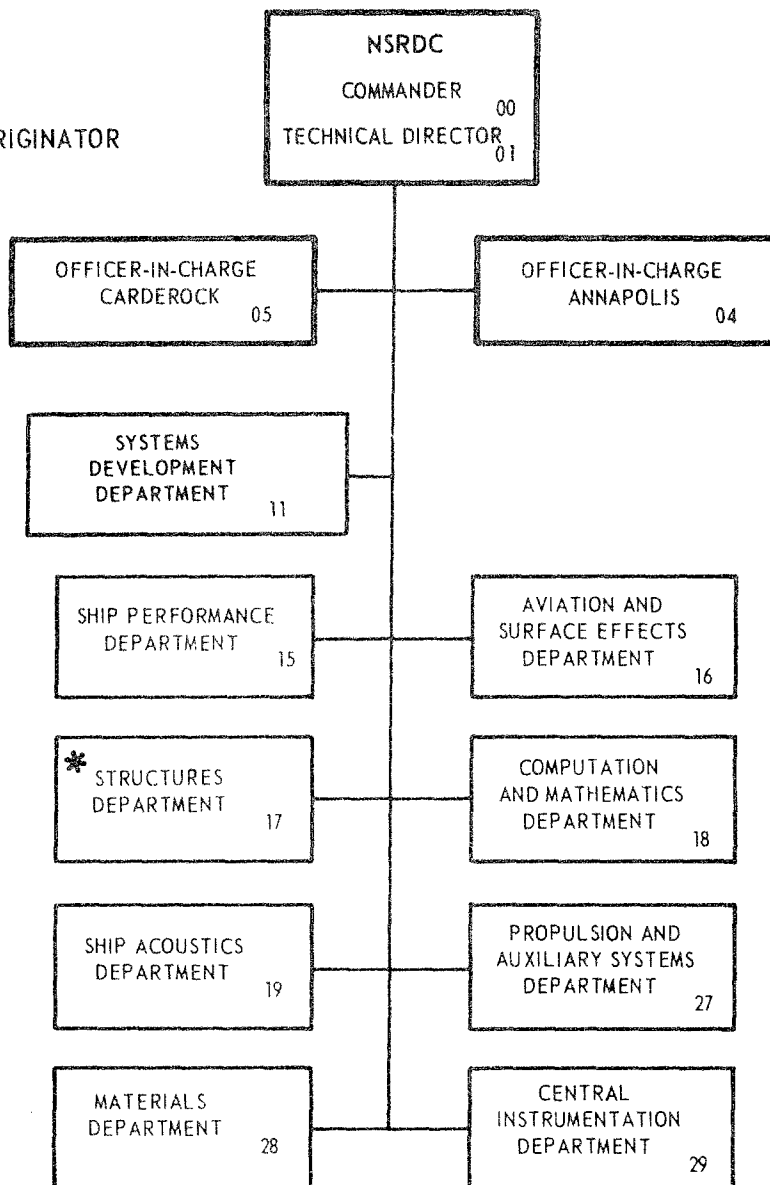
SLAMMING TESTS OF THREE-DIMENSIONAL MODELS IN CALM WATER AND WAVES

The Naval Ship Research and Development Center is a U. S. Navy center for laboratory effort directed at achieving improved sea and air vehicles. It was formed in March 1967 by merging the David Taylor Model Basin at Carderock, Maryland with the Marine Engineering Laboratory at Annapolis, Maryland.

Naval Ship Research and Development Center
Bethesda, Md. 20034

MAJOR NSRDC ORGANIZATIONAL COMPONENTS

*REPORT ORIGINATOR



DEPARTMENT OF THE NAVY
NAVAL SHIP RESEARCH AND DEVELOPMENT CENTER
BETHESDA, MARYLAND 20034

SLAMMING TESTS OF THREE-DIMENSIONAL MODELS
IN CALM WATER AND WAVES

by

Sheng-Lun Chuang



APPROVED FOR PUBLIC RELEASE: DISTRIBUTION UNLIMITED

September 1973

Report 4095

TABLE OF CONTENTS

	Page
ABSTRACT	1
ADMINISTRATIVE INFORMATION	1
INTRODUCTION	1
PREDICTION OF SLAMMING PRESSURE	2
TEST METHOD	6
DESCRIPTION OF MODELS	6
TEST PROCEDURE	6
INSTRUMENTATION SYSTEM	7
TEST RESULTS AND DISCUSSION	7
IMPACT IN CALM WATER	7
IMPACT IN WAVES	12
ELASTICITY EFFECT	14
SUMMARY AND CONCLUSIONS	16
IMPACT IN CALM WATER	16
IMPACT IN WAVES	16
ELASTICITY EFFECT	17
ACKNOWLEDGMENTS	17

LIST OF FIGURES

Figure 1 — Comparison of Maximum Impact Pressures as Determined by Various Models	18
Figure 2 — Velocity Diagram	18
Figure 3 — The Three-Dimensional Models Utilized for the Tests	19
Figure 4 — Details of Test Facility	19

	Page
Figure 5 – Calm Water Impact of Three-Dimensional Flat-Bottom Model with Zero Trim and Zero Horizontal Velocity	20
Figure 6 – Maximum Impact Pressure during Calm Water Impact of Three-Dimensional Flat-Bottom Model with 6-Degree Trim and Zero Horizontal Velocity	22
Figure 7 – Maximum Impact Pressure during Calm Water Impact of Three-Dimensional Flat-Bottom Model with 6-Degree Trim and Various Horizontal Velocities	22
Figure 8 – Calm Water Impact of Three-Dimensional Flat-Bottom Model with Zero Trim and Various Horizontal Velocities	23
Figure 9 – Maximum Impact Pressure during Calm Water Impact of Three-Dimensional Flat-Bottom Model with –3 Degree Trim and Zero Horizontal Velocity	25
Figure 10 – Maximum Impact Pressure during Calm Water Impact of Three-Dimensional Flat-Bottom Model with –3 Degree Trim and Various Horizontal Velocities	25
Figure 11 – Effect of Added Weight on Calm Water Impact of Three-Dimensional Flat-Bottom Model with Zero Trim and Zero Horizontal Velocity	26
Figure 12 – Effect of Added Weight on Calm Water Impact of Three-Dimensional Flat-Bottom Model with Zero Trim and 10-Knot Horizontal Velocity	28
Figure 13 – Maximum Impact Pressure during Calm Water Impact of Three-Dimensional Varying-Deadrise Angle Model with Zero Trim and Zero Horizontal Velocity	30
Figure 14 – Maximum Impact Pressure during Calm Water Impact of Three-Dimensional Varying-Deadrise Angle Model with 6-Degree Trim and Zero Horizontal Velocity	30
Figure 15 – Maximum Impact Pressure during Calm Water Impact of Three-Dimensional Varying-Deadrise Angle Model with 6-Degree Trim and Various Horizontal Velocities	31
Figure 16 – Maximum Impact Pressure during Calm Water Impact of Three-Dimensional Varying-Deadrise Angle Model with Zero Trim and Various Horizontal Velocities	32
Figure 17 – Maximum Impact Pressure during Calm Water Impact of Three-Dimensional 10-Degree Model with Zero Trim and Zero Horizontal Velocity	32
Figure 18 – Maximum Impact Pressure during Calm Water Impact of Three-Dimensional 10-Degree Model with 6-Degree Trim and Zero Horizontal Velocity	33
Figure 19 – Maximum Impact Pressure during Calm Water Impact of Three-Dimensional 10-Degree Model with 6-Degree Trim and Various Horizontal Velocities	33
Figure 20 – Maximum Impact Pressure during Calm Water Impact of Three-Dimensional 10-Degree Model with Zero Trim and Various Horizontal Velocities	34

Figure 21 – Maximum Impact Pressure during Calm Water Impact of Three-Dimensional 10-Degree Model with –3 Degree Trim and Various Horizontal Velocities	34
Figure 22 – Comparison of Predicted and Experimental Results for Various Models in Waves	35
Figure 23 – Elasticity Effect on Maximum Impact Pressure of the Three-Dimensional Varying-Deadrise Angle Model	36
Figure 24 – Elasticity Effect on Maximum Impact Pressure of the Three-Dimensional 10-Degree Model	39

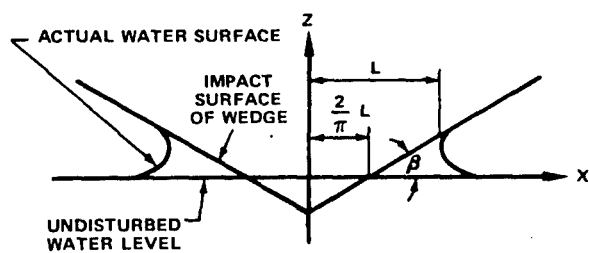
LIST OF TABLES

Table 1 – Comparison of Experimental and Predicted Slamming Pressures for Flat-Bottom Model in Waves	42
Table 2 – Comparison of Experimental and Predicted Slamming Pressures for 10-Degree Model in Waves	45
Table 3 – Comparison of Experimental and Predicted Slamming Pressures for Varying-Deadrise Angle Model in Waves	47

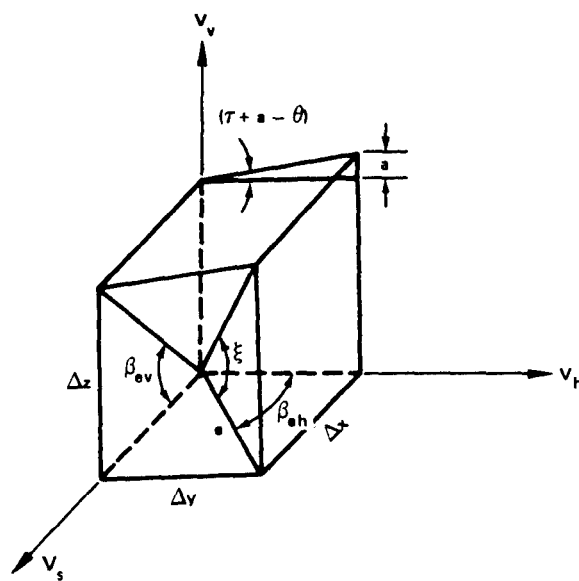
NOTATION

c_{zz}	Damping constant of fluid
D	Dimensional, e.g., 2-D = two dimensional, 3-D = three dimensional
h_w	Wave height from crest to trough
k	Arbitrary constant
k_{zz}	Spring constant of fluid
L	Half wetted breadth of wedge measured horizontally; see Sketch A at the end of the notation
L_w	Wave length
m_{zz}	Added mass of fluid
p_a	Interacting pressure
p_i	Impact pressure
p_p	Planing pressure
p_r	Rigid body pressure
p_t	Total pressure ($p_i + p_p$)
T_w	Wave period
V_h	Horizontal velocity
V_n	Normal velocity to wave surface
V_{ns}	Normal velocity to impact surface of craft
V_t	Tangential velocity to wave surface
V_{ts}	Tangential velocity to impact surface of craft
V_v	Vertical velocity
V_w	Wave celerity
w	Deflection of impact surface
\dot{w}	$= dw/dt$
\ddot{w}	$= d^2 w/dt^2$
y	Percent of L_w from positive θ_{\max}
α	Buttock angle
β	Deadrise angle
β_{eh}	Angle on wave surface measured from forward longitudinal direction to the plane normal to wave surface and impact surface on hull bottom at a point of concern; see Sketch B

β_{ev}	Angle on transverse plane normal to wave surface and measured from impact surface on hull bottom to wave surface; see Sketch B
θ	Wave slope
θ_{\max}	Maximum wave slope
ξ	Effective impact angle on plane normal to wave surface and impact surface on hull bottom measured from wave surface to impact surface of hull bottom; see Sketch B
ρ	Mass density of fluid
τ	Trim angle



Sketch A



Sketch B

ABSTRACT

A prediction method is being developed at the Naval Ship Research and Development Center (NSRDC) for determining wave impact loads when a high-performance vehicle experiences slamming while traveling at very high speeds. This method is based on the Wagner wedge impact theory, the Chuang cone impact theory, and NSRDC drop tests of wedges and cones. Determination of impact velocity is based on the hypothesis that it is equal to the relative velocity between the impact surface of the moving body and the wave surface. As part of the development of this prediction method, slamming tests of three-dimensional models were conducted in calm water and waves, and the results were recorded during the time of impact when the model traveled with both horizontal and vertical velocities. The agreement between experimental and predicted results was remarkably good. The effect of elasticity on slamming was also investigated during the tests. As expected, results clearly indicated a reduction in impact pressure due to elasticity effect.

ADMINISTRATIVE INFORMATION

This investigation was carried out at the Naval Ship Research and Development Center (NSRDC) during fiscal year 1971 as part of a general study on slamming under the Surface Effect Ships Program. The work was funded by the Surface Effect Project Office (PM 17). Funds for the publication of this report were provided under Work Unit 4-1700-001.

INTRODUCTION

Developmental studies of a high-performance vehicle have been concerned with the problem of slamming. While attempting to maintain its high speed (for instance, 50 to 100 knots and more) during heavy weather, a high-performance vehicle inevitably experiences at its bow or elsewhere the impact force of the surface wave of the sea. This type of impact force, usually designated as "ship slamming," can easily damage the local hull structure or cause the entire hull to vibrate.

In order to determine slamming damage to hull structures, NSRDC has conducted basic impact tests of two-dimensional models in calm water¹ and seakeeping tests of three-dimensional models in waves.² However, the information provided by those tests was insufficient to enable predictions of impact pressure in the slamming area of the high-speed high-performance vehicle; horizontal velocity was low in the seakeeping tests and was omitted for the two-dimensional models.

¹Chuang, S.L., "Investigation of Impact of Rigid and Elastic Bodies with Water," NSRDC Report 3248 (Feb 1970).

²Ochi, M.D. and J. Bonilla-Norat, "Pressure-Velocity Relationship in Impact of a Ship Model Dropped onto the Water Surface and in Slamming in Waves," NSRDC Report 3153 (Jun 1970).

Experimental data on the slamming of three-dimensional models were thus required in order to evaluate the accuracy of the method being developed^{3,4} at NSRDC for predicting the three-dimensional slamming pressure in waves.

The objectives of the present work are:

1. To complete the development of the method for predicting the slamming loads of high-performance vehicles traveling at high horizontal velocities in waves.
2. To perform three-dimensional slamming tests for comparison with predicted results.
3. To investigate the effect of deformable impact surface on slamming pressure.

This work is a continuation of NSRDC slamming research and is particularly applicable to the determination of slamming loads for the design of hulls of high-speed, high-performance vehicles.

PREDICTION OF SLAMMING PRESSURE

In determining the slamming of a high-speed craft, the pressure that acts normal to the hull bottom in the slamming area may be separated into two components:

1. The impact pressure p_i due to the velocity component of the craft normal to the wave surface
2. The planing pressure p_p due to the velocity component of the craft tangential to the wave surface.

To estimate the maximum impact pressure $\text{Max } p_i$, the pressure-velocity relation may be expressed in the general form of

$$\text{Max } p_i = k \rho V_n^2 \quad (1)$$

where k is an arbitrary constant,

ρ is the mass density of fluid in pounds-second² per feet⁴,

V_n is the normal velocity to the wave surface in feet per second,
and the impact pressure p_i is in pounds per square inch.

³Chuang, S.L., "Impact Pressure Distributions on Wedge-Shaped Hull Bottoms of High-Speed Craft," NSRDC Report 2953 (Aug 1969).

⁴Chuang, S.L., "Design Criteria for Hydrofoil Hull Bottom Plating," NSRDC Report 3509 (Jan 1971).

The values of k for wedges and cones can be determined from the Wagner wedge impact theory,⁵ the Chuang cone impact theory,⁶ and NSRDC drop tests of wedges and cones.⁷ When the impact angles ξ are small, the k values determined by these different methods deviate considerably, especially the comparisons between theoretical and experimental values; see Figure 1. Therefore, it is reasonable to believe that the experimental values are more realistic. Moreover, since the three-dimensional hull form is within the limits of wedge-shaped and cone-shaped bodies, the k values for the impact of high-performance vehicles may be approximated by the dotted line shown in Figure 1. This dotted line can be expressed by equations obtainable by the method of curve fitting.⁸ These equations are:

$$\begin{aligned}
 &1. \text{ For } 0 \leq \xi < 2.2 \text{ deg:} \\
 &\quad k = 0.045833 \xi^2 + 0.149167 \xi + 0.32 \\
 &2. \text{ For } 2.2 \leq \xi < 11 \text{ deg:} \\
 &\quad k = 2.1820894 - 0.9451815 \xi + 0.2037541 \xi^2 \\
 &\quad \quad - 0.0233896 \xi^3 + 0.0013578 \xi^4 - 0.00003132 \xi^5 \\
 &3. \text{ For } 11 \leq \xi < 20 \text{ deg:} \\
 &\quad k = 4.748742 - 1.3450284 \xi + 0.1576516 \xi^2 \\
 &\quad \quad - 0.0092976 \xi^3 + 0.0002735 \xi^4 - 0.00000319864 \xi^5 \\
 &4. \text{ For } 20 \text{ deg} \leq \xi \text{ (Modified Wagner Formula):} \\
 &\quad k = (1 + 2.4674 / \tan^2 \xi) 0.76856471 / 288
 \end{aligned} \tag{2}$$

The effective impact angle ξ may be calculated from^{3,4}

$$\tan \xi = \cos \beta_{eh} \tan (\tau + \alpha - \theta) + \sin \beta_{eh} \tan \beta_{ev} \tag{3}$$

with β_{eh} and β_{ev} given by

⁵Wagner, V.H., "Über Stosz- und Gleitvorgänge an der Oberfläche von Flüssigkeiten," Zeitschrift für Angewandte Mathematik und Mechanik, Vol. 12, No. 4, pp. 193-215 (Aug 1932).

⁶Chuang, S.L., "Theoretical Investigations on Slamming of Cone-Shaped Bodies," Journal of Ship Research, Vol. 13, No. 4 (Dec 1969).

⁷Chuang, S.L. and D.T. Milne, "Drop Tests of Cones to Investigate the Three-Dimensional Effects of Slamming," NSRDC Report 3543 (Apr 1971).

⁸Carnahan, B. et al., "Applied Numerical Methods," John Wiley & Son, Inc., New York (1969), Chapter 1.

$$\left. \begin{aligned} \tan \beta_{eh} &= \frac{\tan \beta}{\sin (\tau - \theta) + \tan \alpha \cos (\tau - \theta)} \\ \tan \beta_{ev} &= \frac{\tan \beta}{\cos (\tau - \theta) - \tan \alpha \sin (\tau - \theta)} \end{aligned} \right\} \quad (4)$$

The planing pressure acting normal to the hull bottom is⁴

$$\text{Max } p_p = \frac{1}{2} \rho V_t^2 \cos \beta_{eh} (1/144) \quad (5)$$

The total pressure due to velocity components of the craft both normal and tangent to the wave surface is therefore

$$p_t = p_i + p_p \quad (6)$$

In Equations (3) to (6), τ is the trim angle, α is the buttock angle, θ is the wave slope, β is the dead-rise angle, β_{eh} is the effective impact angle in the horizontal longitudinal plane, β_{ev} is the effective impact angle in the vertical transverse plane, V_t is the tangential velocity in feet per second, and the total pressure p_t is in pounds per square inch. The unit for the angle measurement can be either in degrees or in radians as required in the equations. The value of the mass density of fluid ρ is simply the unit weight of fluid divided by the gravitational acceleration g , e.g., 62.4/ g for fresh water and 64/ g for sea water.

The values for V_n in Equation (1) and V_t in Equation (6) may be determined in the following manner. Consider that the craft moves with a horizontal velocity V_h and a vertical velocity V_v ; at the time of impact, the craft has a trim angle τ and a buttock angle α . As indicated in Figure 2, both V_h and V_v can be separated into two velocity components, one normal and one tangential to the impact surface of the craft. Since nonviscous fluid is assumed, no pressure is generated due to the tangential velocity component. In the actual case, the tangential velocity produces a resistance or drag force. Since this force is parallel to the impact surface, it does not generate a slamming pressure. In other words, only the normal velocity component will generate the slamming pressure as the craft strikes the wave surface. This normal velocity V_{ns} is

$$V_{ns} = V_v \cos (\tau + \alpha) + V_h \sin (\tau + \alpha) \quad (7)$$

and it is to be further separated into a component normal to the wave surface and a component tangential to the wave surface. The wave length (in feet) is L_w , the wave height (in feet) is h_w , the wave slope is θ , the wave celerity (in feet per second) is V_w , and the wave period (in seconds) is T_w . If a harmonic deep-water wave of finite height is assumed, the surface of the sea can be described mathematically as having the

$$\left. \begin{aligned}
 V_w &= 2.26 \sqrt{L_w} \text{ (feet per second)} \\
 \theta &= \theta_{\max} \cos \frac{2\pi}{L_w} y \text{ (radians)} \\
 \theta_{\max} &= \frac{2\pi}{L_w} \frac{h_w}{2} \text{ (radians)} \\
 T_w &= 0.442 \sqrt{L_w} \text{ (seconds)} \\
 L_w &= 5.12 T_w^2 \text{ (feet)}
 \end{aligned} \right\} \quad (8)$$

Since the pulse of the impact pressure lasts around several milliseconds, the event of impact occurs only at and very near the wave surface of the sea. Therefore, it is reasonable to assume that the impact velocity is equal to the relative velocity between the impact surface of the moving body and the wave surface. Based on this hypothesis and with the wave surface moving with the wave celerity V_w , the relative normal velocity of the impact surface to the wave surface is

$$\left. \begin{aligned}
 V_n &= [V_{ns} + V_w \sin(\tau + \alpha)] \cos(\tau + \alpha - \theta) \\
 V_t &= [V_{ns} + V_w \sin(\tau + \alpha)] \sin(\tau + \alpha - \theta)
 \end{aligned} \right\} \quad (9)$$

Since the V_n used for estimating the impact pressure by Equation (1) has been referred to V_v for Equations (2) to (4) when the wave slope θ is zero, it is necessary to divide V_n by $\cos^2(\tau + \alpha)$ so that Equations (1) to (4) can be used for the present prediction of craft slamming pressure. Then, the combination of Equations (9) and (7) becomes

$$\left. \begin{aligned}
 V_{ns} &= V_v \cos(\tau + \alpha) + (V_h + V_w) \sin(\tau + \alpha) \\
 V_n &= V_{ns} \cos(\tau + \alpha - \theta) / \cos^2(\tau + \alpha) \\
 V_t &= V_{ns} \sin(\tau + \alpha - \theta)
 \end{aligned} \right\} \quad (10)$$

If the slamming occurs during the time when there is no wave and no horizontal velocity of the craft, then $V_h = 0$, $V_w = 0$, and $\theta = 0$; Equation (10) becomes

$$V_{ns} = V_v \cos (\tau + \alpha)$$

$$V_n = V_v \cos^2 (\tau + \alpha) / \cos^2 (\tau + \alpha)$$

$$\equiv V_v$$

This means that V_n becomes identical to V_v , which was used previously for the prediction of the impact pressure of wedges and cones.^{1,7}

TEST METHOD

DESCRIPTION OF MODELS

Three three-dimensional models were tested; one had a flat bottom, one a bottom with a 10-deg deadrise angle, and one a bottom with deadrise angles varying from 0 deg at the stern to 20 deg at the bow. These models are shown in Figure 3.

The flat bottom model had a 3/8-in. aluminum bottom plate, with gage locations as shown in the figure. The other two models were constructed of 3/8-in. aluminum plate on the starboard side and 1/16-in. aluminum sheet on the port side to enable the elastic effect of the bottom to be examined from the slamming test records.

TEST PROCEDURE

Tests were conducted with Carriage 5 (maximum capability of 55 knots) in the NSRDC high-speed towing basin. Figure 4 shows details of the test assembly. The releasing mechanism consisted of a solenoid attached to the cross beam by an adjustable steel rod; this could be raised or lowered for the proper drop height of the model. The solenoid was equipped with a hook for hanging the model. When the solenoid was activated, the hook was very quickly released, and the model fell freely in the vertical direction along the guide rails. The total drop weight of the drop-gear assembly and the model shown in the figure was 290 lb for each model tested.

The drop heights ranged from 3 to 18 in. and the horizontal velocity from 0 to 45 knots. Pressures, accelerations, deflections, vertical displacement, and velocities of the moving model were recorded. In addition, 16-mm high-speed movies were taken for selected runs at film speeds varying up to approximately 1000 frames/sec.

INSTRUMENTATION SYSTEM

The instrumentation system consisted essentially of quartz-crystal transducers, charge amplifiers, d-c amplifiers, and a tape recorder. The validity of the pressure measurements of the complete recording system was tested electronically and mechanically; the system was also calibrated by means of an underwater explosion. The results indicated that the entire recording system had the ability to pick up and record any high-frequency acoustic pressure that was present during the impact of the falling body with the water surface. A detailed description of the instrumentation has already been published; see Appendix A in Chuang and Milne.⁷ In addition, a sonic probe was installed at the towing carriage for measuring wave profiles during the course of model impact in waves.

TEST RESULTS AND DISCUSSION

Test results are presented and discussed in relation to the objectives stated in this report. The results are presented separately for the three general areas: the impact of the models in calm water, the impact of the models in waves, and the effect of deformation of impact surface on the impact pressure of the models.

IMPACT IN CALM WATER

Flat-Bottom Model with Zero Trim and Zero Horizontal Velocity

Test results are shown for the maximum impact pressures (Figure 5a), the maximum impact accelerations (Figure 5b), the maximum plate deflections (Figure 5c) measured during the impact. The prediction line is also plotted in Figure 5a for comparison with maximum pressures; the measured pressures were generally less than the predicted values. Reasons for these differences are discussed in the following:

1. Since the impact causes the impact surface of the flat-bottom model to deform in its elastic region (see Figure 5c) the measured maximum pressure p_t actually consists of two types of pressures: (1) a rigid-body impact pressure p_r caused by the impact (as if the impact surface were held rigid) and (2) a relief interacting pressure p_a which reduces the total impact pressure p_t so that it is less than the rigid-body impact pressure p_r . The predicted pressure is based on rigid body response. This phenomenon has previously been established from several tests.¹

2. The weight per unit impact area for the present flat-bottom model was only 41.5 psi, which is comparatively light. Thus, the measured maximum impact pressure would be expected to be lower than the predicted value.

3. The maximum impact pressure is also related to the maximum impact deceleration. For the same drop height or impact velocity, the higher the maximum impact deceleration (i.e., acceleration in the pressure relief direction), the lower the maximum impact pressure that may be expected. This is illustrated in Figure 5b. As indicated there, the impact of the present flat-bottom model produced the highest impact acceleration and thus had the lowest impact pressure.

Flat-Bottom Model with 6-Degree Trim (Bow up) and Zero Horizontal Velocity

Figure 6 gives the test results for the maximum impact pressure. The impact accelerations and plate deflections were not plotted because they were negligibly small and not readable. Because both acceleration and deflection readings were negligibly small, the maximum impact pressure can be predicted rather accurately either from present prediction methods or from cone-impact test results. In this case the line from cone-test results gives a better fit of the present test results. Both prediction lines are included in Figure 6.

Flat-Bottom Model with 6-Degree Trim and Various Forward Velocities

The forward velocities for this case were 5, 10, 15, and 20 knots. The test results (Figure 7) are considered very good when compared to the predictions. The acceleration and deflection measurements were again very small. This is the first time that experimental results have been available to compare with the predictions of three-dimensional slamming including both the horizontal and vertical velocities. Although these comparisons have been very good, further checks are still needed in order to build up confidence in the three-dimensional slamming prediction. Other tests were therefore performed to build up this confidence.

Flat-Bottom Model with Zero Trim and Various Forward Velocities

The objective here was to demonstrate that the impact pressure would not be affected by a change in forward velocities if the impact surface of the moving body and the direction of forward velocity were parallel to the calm-water surface. Only forward velocity has its velocity component parallel to the impact surface of the moving body; its normal velocity component to the impact surface is zero. Thus, a change in forward velocity will not alter the magnitude of impact pressure if the vertical velocities remain the same.

The results indicated that the maximum impact pressures (Figure 8a), impact accelerations (Figure 8b), and plate deflection (Figure 8c) caused by impact were not affected by changes in forward horizontal velocities. The prediction method also indicated the independence of the forward horizontal velocities; see Figure 8a. The reasons why the measured results were lower than the predictions have been explained earlier.

Flat-Bottom Model with Negative Trim of 3 Degrees (Bow Down)

The objective was to investigate whether the theory still applied when the flat-bottom model was tested bow downward with a negative trim of 3 deg. First the model was dropped with negative trim but without forward velocity. The test results were compared with both the prediction method and with the test results from the 3-deg cone. As shown in Figure 9, the comparisons gave reasonably good agreement. Since the horizontal velocity of the model was zero during the drop, the trim of the model with bow upward or bow downward does not prove that the theory is applicable to impact with the negative trim of the model. Therefore, the model was dropped again with forward horizontal velocity and had a negative trim of 3 deg. The test results (Figure 10) showed general agreement with values given by the prediction method. When the forward speed of the model goes up, as expected, the impact pressure usually decreases. Because of the yawing instability developed during the test under negative trim conditions, no speed higher than 10 knots was utilized.

Effect on Slamming Pressure of Additional Drop Weight

Results showed no apparent effect on slamming pressure from adding 85 lb to the original 290 lb of drop weight. This was true when the model was dropped without trim and forward speed (Figures 11a—11c) and when it was dropped without trim but with 10 knots of forward speed (Figures 12a—12c). However, this finding cannot be considered conclusive because the added 85 lb is only 29 percent of the original drop weight. Therefore, additional experiments are needed in this area.

Varying Deadrise-Angle Model under Zero Trim and Zero Horizontal Velocity

The impact bottom of the varying deadrise-angle model has 0-deg deadrise at the stern and 20-deg deadrise angle at the bow. Because of this variation, the buttock angle of this model was not zero but

ranged from zero at the keel to maximum at the chine of the model. Calculations indicated that the buttock angle at the gage locations was 1.516 deg. However, at and after the location of the pressure gage at the stern, the deadrise angle was zero and so was the buttock angle. At and forward of the stern pressure gage, the buttock angle was 1.516 deg. Thus the buttock angle can physically be considered to be either zero or 1.516 deg at the location of the stern pressure gage.

Inasmuch as impact pressure is very sensitive to very small deadrise angle of less than 4 deg, a slight change in deadrise angle would change the impact pressure drastically because of the three-dimensional effect and the trapped air phenomenon.¹ Figure 1 clearly indicated the large variation in impact pressures for impacts of wedges and cones (both experimental and theoretical) in the small deadrise-angle region. Therefore, large deviations between measured and predicted values are to be expected within the small deadrise-angle region, especially when the model buttock angle cannot be determined accurately.

Bottom plating of this model consisted of 3/8-in. aluminum plate on the starboard side and 1/16-in. aluminum sheet on the port side; see Figure 3. The test results shown in Figure 13 indicate the maximum impact pressures measured on the 3/8-in. plate side for comparisons with predictions of rigid body impact pressures. The pressures measured on the 1/16-in. sheet side will be presented later in connection with the investigation of elasticity effect.

Measured and predicted values of the maximum impact pressures were compared for deadrise angles of 0, 10, and 20 deg. For the 0-deg deadrise angle, the calculations were made for buttock angles of 0, 0.758, and 1.516 deg.

For this particular series of slamming tests, the predictions were in very good agreement with measurements for a deadrise angle of 0 deg when the mean buttock angle of 0.758 deg was used; see Figure 13. The agreement was also very good for a deadrise angle of 20 deg but predictions were too low for 10 deg. Predictions made using the Wagner theory worked very well for the 10-deg deadrise angle.

Varying Deadrise-Angle Model under 6-Degree Trim and Zero Horizontal Velocity

The method of analysis was similar to previous cases. For the zero deadrise angle, the prediction was better when the mean buttock angle of 0.758 deg was used (Figure 14). Although the predictions were very good for the 20-deg deadrise angle, the readings were too small to read for great accuracy.

Again, the predicted values were lower than the test results for the 10-deg deadrise angle, but not by much.

Varying Deadrise-Angle Model with 6-Degree Trim and Various Horizontal Velocities

The test results are given in Figures 15a and 15b for deadrise angles of 0 and 10 deg, respectively. At the forward speed of the model, the pressure readings were not recorded at the 20-deg deadrise angle because the model was not down far enough for that particular gage location to reach the water.

As indicated in Figure 15a for the 0-deg deadrise angle, each forward speed consisted of a bandwidth for the prediction values with limit values for buttock angles of 0 and 1.516 deg. The agreement between the predictions and the measured results was very good regardless of whether the buttock angle was used for the predictions.

The agreement was also good for the 10-deg-deadrise angle (Figure 15b).

Varying Deadrise-Angle Model with 0-Degree Trim and Various Horizontal Velocities

Again, because of the forward speed, the impact pressure reading at the 20-deg deadrise angle was not recorded for speeds higher than 5 knots due to the fact that the gages were not able to reach the water. Due to turning of the model, speeds higher than 15 knots were not attempted.

According to these limited test results, Figure 16, indicates that the predictions were slightly lower than the test results for 0- and 10-deg deadrise angles.

10-Degree Model with Zero Trim and Zero Horizontal Velocity

The test results are compared in Figure 17 with the Wagner wedge theory,⁵ the Chuang cone theory,⁶ and the wedge-test formula⁷ and three-dimensional prediction formulas. The Chuang cone theory gave the best prediction of the test results.

10-Degree Model with 6-Degree Trim and Zero Horizontal Velocity

The test results are given in Figure 18 together with three-dimensional and cone theory predictions. The 3-D prediction was slightly lower than the test results but the cone theory was in good agreement with the measured values.

10-Degree Model with 6-Degree Trim and Various Horizontal Velocities

The combination of 10-deg-deadrise angle and 6-deg trim enabled the model to be tested at very high forward speeds and this part of the test was run up to 45 knots. Even at such a high horizontal speed, the agreement between the test results and the predictions were still very good; see Figure 19.

10-Degree Model with Zero Trim and Various Horizontal Velocities

Because the model showed instability as it speeded up, the horizontal velocity was limited to 15 knots. As indicated previously, there was no influence on impact pressure by the horizontal velocity. This phenomenon is shown in Figure 20.

10-Degree Model with Negative 3-Degree Trim (Bow down) and Various Forward Horizontal Velocities

The model stability was worse than when it was towed with zero trim; therefore it was tested at speeds no higher than 7 knots. As can be seen from Figure 21, the higher the forward speed, the more difficult the measurement of impact pressure. The predictions show slightly lower pressures than do the test results. However, they do show the evidence that the higher the forward speed, the more difficult the prediction of impact pressure.

Summary for Calm Water Impact

The detailed testing of the three models established confidence that the present method gave reasonably good predictions of the slamming pressures during impact of a three-dimensional hull form in calm water.

IMPACT IN WAVES

The following items were measured, recorded, or calculated during the impact tests of the models in waves:

Wave height h_w

Wave period T_w

Forward speed of model V_h

Vertical velocity of model V_v

Vertical displacement of model from hanging position

Acceleration at impact surface (see Figure 3)

Deflection of impact surface where acceleration and pressure are measured (see Figure 3)

Deadrise angle β

Buttock angle α

Trim angle τ

Location of impact point in wave surface

Wavelength was calculated from the equation $L_w = 5.12 T_w^2$ (Chuang⁴). Other necessary calculations were mostly based on the formulas given in Chuang.^{3,4}

The information obtained from the tests enabled the impact pressure to be calculated by the prediction method. The comparisons between the calculated and recorded values of the impact pressures are given in Tables 1 through 3 for the three models. Considering the many variables previously listed, the agreement is considered very good. Because the wavemeter was located several feet away from the model, there was some discrepancy between the measured wave profile and the wave profile at the point of impact by the model.

Calculations were made for the varying-degree model with assumed α values of 0, 0.76, and 1.52 deg at $\beta = 0$. This was done because the gage was located where the buttock angle could be considered to be any one of these three values. Since the prediction for a small impact angle is very sensitive to changes in that angle, a slight change in α would change the p_t value drastically, for example, for Run 142 with $\beta = 0$, $\tau = 0$:

Assumed	Calculated
$\alpha = 0$ deg	$p_t = 42.32$ psi
$\alpha = 0.76$ deg	$p_t = 61.85$ psi
$\alpha = 1.52$ deg	$p_t = 88.20$ psi

However, examination of the test results indicated that the mean value of $\alpha = 0.76$ deg usually gave the best predictions. As indicated in Tables 1–3, the calculated planing pressure p_p was much smaller than the calculated impact pressure p_t . This suggests that the planing pressure p_p may be omitted without introducing serious error.

Tables 1–3 also give the calculated k values from the equation

$$\text{Recorded Max } p_t \approx \text{Recorded Max } p_i = k \rho V_n^2 \quad (2)$$

Figure 22 compares these k values with the prediction line for the three-dimensional slamming. Several points are worth mentioning.

1. The angles of impact ξ are not necessarily the deadrise angles of the model β . If β is small, the differences between β and ξ are large; if β is large, their differences become small.
2. Except for 1- to 2-deg angles of impact ξ , predictions agree very well with results obtained from present tests. However, the test results of cones agreed very well with the upper limit of the k values for 1 to 2 deg of ξ .
3. The present test showed that the k values varied considerably for 1 to 2 deg of ξ . This is attributed to the fact that the trapped-air phenomenon comes into play for small angles of impact, say 1 to 2 deg. During the impact of such a small angle, the air may or may not become entrapped. If the air is entrapped, the k values will be reduced to very small values. If however the air escapes completely before the impact, the k values will be very large. As indicated in Figure 22, the k values for 1 to 2 deg of ξ ranged from as low as 0.18 to as high as 1.39.
4. A last point, although obvious, is worth mentioning, namely that the angle of impact ξ depends not only on the deadrise angle β but also on the trim angle τ , the buttock angle α of the model (or ship), and the wave slope θ . Moreover, the impact velocity depends on the vertical and horizontal velocities of the model and on the wave velocity. This impact velocity is also influenced by β , τ , α of the model and θ of the wave. Therefore, it is insufficient to make predictions on impact pressures based only on the deadrise angle β and the vertical velocity of the model (or ship).

ELASTICITY EFFECT

Slamming loads originate at the impact surface between the impact body and the water surface. If the impact surface deforms during the process of impact within the time duration of the impact pressure pulse, then this pressure pulse will be affected. Usually the impact pressure will be reduced. A general equation for this process is¹

$$\begin{aligned} p_t &= p_r + p_a \\ &= p_r - (m_{zz} \ddot{w} + c_{zz} \dot{w} + k_{zz} w) \end{aligned} \quad (11)$$

where p_t is the total impact pressure generated by the deformable body falling upon the water surface. This p_t can be separated into two types of pressure. The first may be called the rigid body impact pressure p_r , generated by the deformable body as if it were held rigid during impact. The second may be called the interacting pressure p_a caused by interaction between the surface movement of the deformable body and the surrounding water, with or without a thin layer of trapped air between the surfaces.

The interacting pressure p_d may be divided into pressures due to the effects of the inertial, damping, and spring forces of both the trapped air and the water. However, the effects of the forces of trapped air are small compared with those of water and can be neglected. Therefore, Equation (11) applies to the slamming of rigid or deformable bodies with or without entrapped air. The negative sign is used at the right side of the equation because the interacting pressure is always acting against the movement of the impact surface.

For rough estimation of the effect of elasticity, both c_{zz} and k_{zz} may be ignored. Equation (11) then becomes

$$p_t = p_r - m_{zz} \ddot{w}$$

where m_{zz} is the added mass of fluid and may be estimated by the classical formula

$$m_{zz} = \frac{\pi}{2} \rho L^2$$

The accelerations measured for the present flat-bottom model (Figure 5b) were higher than for the circular and the rectangular plate models; the impact pressures were thus lower. However, the increased acceleration for the present flat-bottom model is partly attributed to the rigid-body response of models with lighter weights than those of the other two models. Since the flat-bottom model was not as rigid as the other two models, it was possible to record deflection measurements. Therefore, the reduced impact pressures of the flat-bottom model were also partly caused by the elasticity effect of the model deflection.

Since rigid-body acceleration was not measured for the present flat-bottom model, it is impossible to separate the measured acceleration into one measurement due to the rigid body motion and one due to the elasticity effect. The 10-deg and the varying-deadrise angle models had one side with relatively rigid impact surfaces and one side with relatively elastic impact surfaces. The reductions in impact pressures of elastic surfaces over those of the rigid surface are shown in Figure 23 for the varying-deadrise angle model and in Figure 24 for the 10-deg model.

These figures clearly indicate that the reduction in impact pressure due to the elasticity effect is somewhere between 10 and 25 percent. At the present state-of-the-art, however, a quasi-static approximation is sufficient to meet the immediate needs for the practical design of a hull bottom that will be subjected to slamming. Since the prediction of slamming pressure at the present time can hardly be better than 25 percent of error, neglecting the elasticity effect might be considered a safety margin of the design.

SUMMARY AND CONCLUSIONS

Previous NSRDC studies on slamming have involved drop tests for two-dimensional cases. The present study covers the three-dimensional aspect; its effects on slamming pressure were studied when both vertical and the horizontal impact velocities were involved.

Tests were conducted on three models which had three-dimensional hull forms; one had a flat bottom, one had a 10-deg deadrise-angle bottom, and one had a bottom with deadrise angles that varied from 0 deg at the stern to 20 deg at the bow; see Figure 3. These models were tested under different horizontal and vertical velocities, different trims, and different weights. The objectives of the tests were:

1. To verify experimentally the prediction method given here as part of this study for determining the slamming pressure of a ship bottom in calm water and waves.
2. To determine experimentally the effects of elasticity on slamming pressure and local response of the hull bottom.

On the basis of this series of experimental investigations, the following conclusions have been drawn.

IMPACT IN CALM WATER

The given prediction method predicts the slamming pressure reasonably well for the calm-water impact of a three-dimensional hull form, involving both horizontal and vertical velocities of the craft. The predictions gave slightly lower values than were achieved by the tests for a 10-deg deadrise angle of the hull bottom. However, the test results agreed very well with the cone impact theory⁶ for the impact bottom with 10-deg deadrise angle when the model had no forward horizontal velocity.

IMPACT IN WAVES

Considering the many variables required to determine the slamming pressure in waves, the agreement between the test results and the predictions is considered very good. The following additional findings have been verified experimentally:

1. The value of the impact angle ξ is affected not only by the deadrise angle β , but also by the trim τ , the buttock angle α , and the wave slope θ . Therefore, the impact angle ξ is not necessarily the deadrise angle of hull bottom β .
2. Because of the nature of the trapped air phenomenon, the test results for slamming pressures exhibited considerable scatter for small impact angle ξ . If impact occurred while air was entrapped, the measured pressures were small. If impact occurred after the trapped air had escaped, the measured pressures were large. However, values of measured pressure were still within the range of the impact tests result for cones; see Figure 22.

ELASTICITY EFFECT

The experiments clearly indicated the reduction of slamming pressure when the impact surface was deformable. At the present state-of-the-art for metal structure, this elasticity effect can be regarded as a safety margin by assuming the hull bottom to be a rigid body.* Therefore, the quasi-static approach is sufficient to meet the immediate needs for the practical design of a hull bottom that will be subjected to slamming.

In summary, the prediction method developed here is sufficiently accurate to predict the slamming pressure of a hull bottom during high-speed operation in waves for both rigid and deformable body impacts. This method is based on the Wagner wedge impact theory, the Chuang cone impact theory, and drop tests of wedges and cones performed at NSRDC.

ACKNOWLEDGMENTS

This project was a team effort that involved many people. The detailed design of the models was undertaken by the Mechanical System Division under the supervision of Mr. L.M. Burgee, who assigned Mr. A.R. Synstad to act as principal designer. The construction of the models was performed by the Shop Division and involved personnel of the Planning, Estimating, and Scheduling Section, the Machining Section; the Metal Working Trades Section; the Woodworking Section; and the Paint Shop. The test facility was operated and maintained by the Ship Performance Department under the supervision of Mr. G.J. Milward. The instrumentation system was developed under the supervision of Mr. D.T. Milne and his assistants, Messrs. D.R. Armstrong and H.O. Snoots. Since the tests were conducted in two shifts per day, half of the tests were supervised by Mr. E.A. Zwenig. The motion picture photography was performed by Mr. B.C. Ball and his assistant, Mr. H. Gardner, and some of the data analyses were performed by Mr. A.J. Furio. The author gratefully acknowledges their helpful assistance and valuable suggestions.

Appreciation is also expressed to Mr. A.B. Stavovy and Dr. M.E. Lunchick for their support and all possible assistance in evaluating three-dimensional impact theory from this series of experiments.

*This, of course, would not give a very good approximation for a very flexible hull bottom, e.g., one made of elastomeric material.

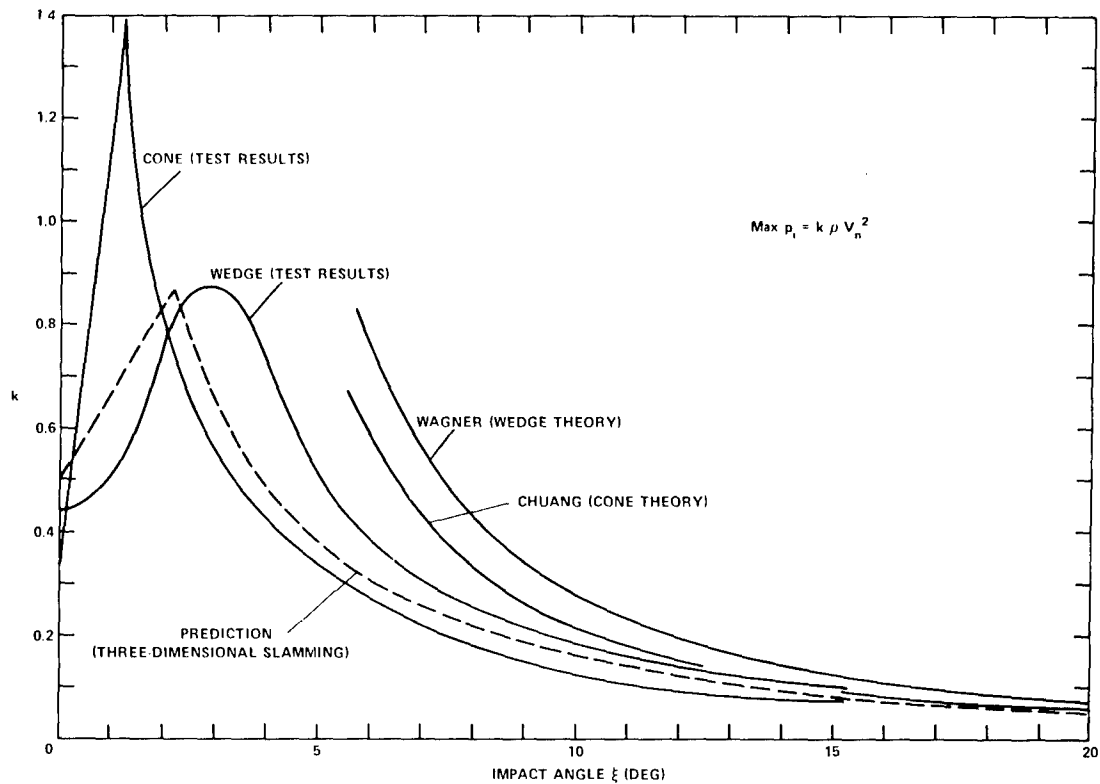


Figure 1 – Comparison of Maximum Impact Pressures as Determined by Various Methods

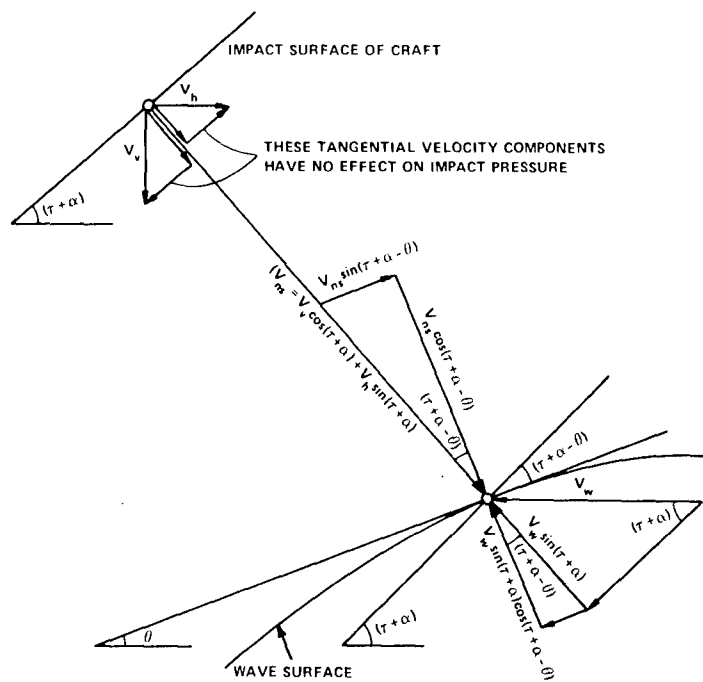


Figure 2 – Velocity Diagram

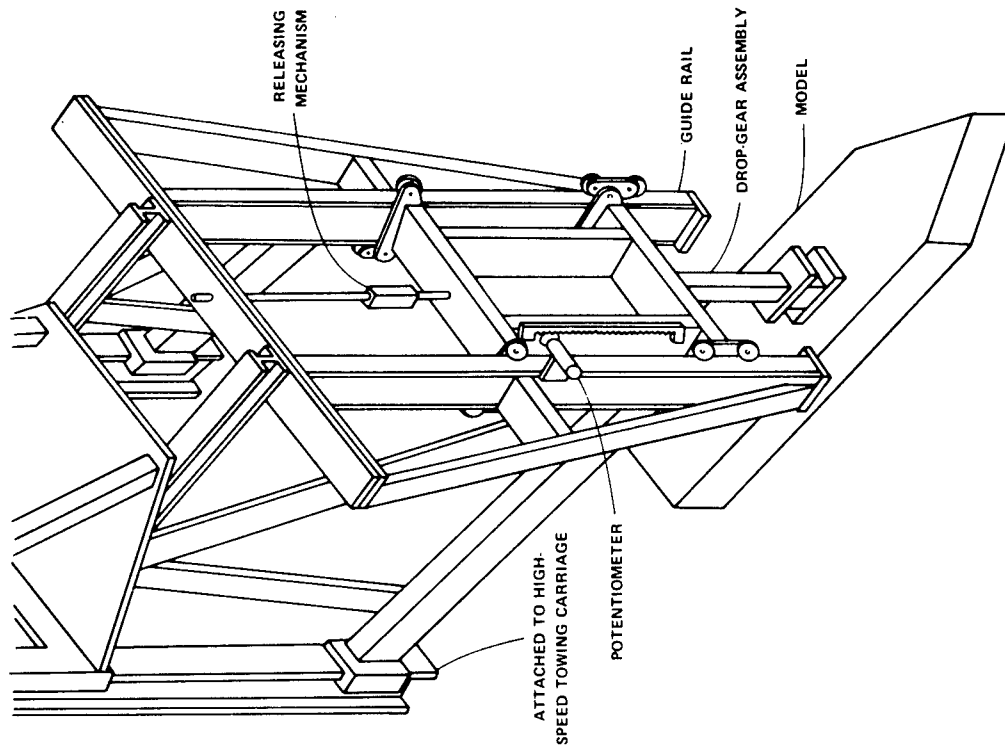


Figure 4 -- Details of Test Facility

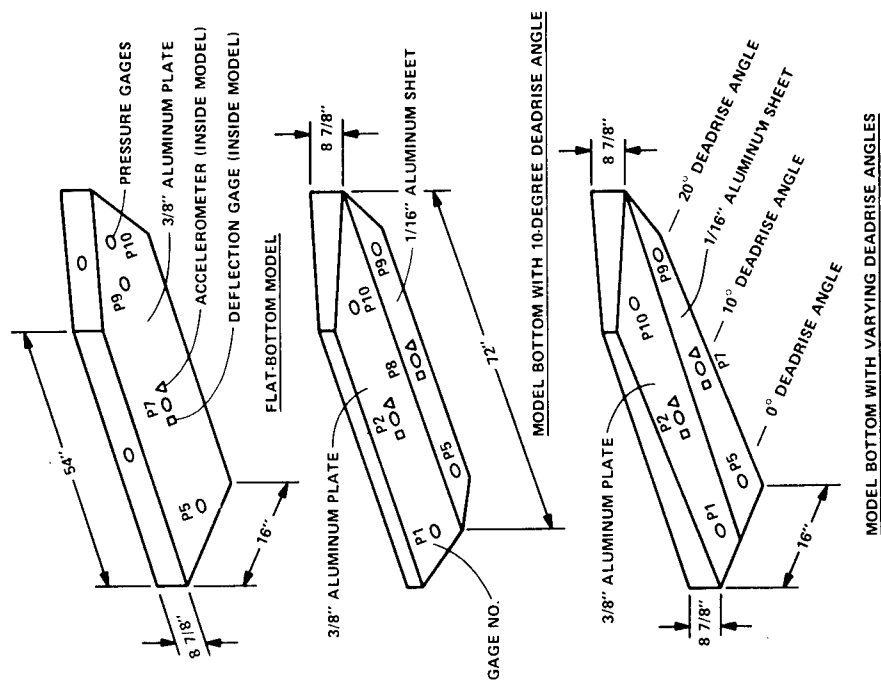


Figure 3 -- The Three-Dimensional Models Utilized for the Tests

Figure 5 -- Calm Water Impact of Three-Dimensional Flat-Bottom Model with Zero Trim and Zero Horizontal Velocity

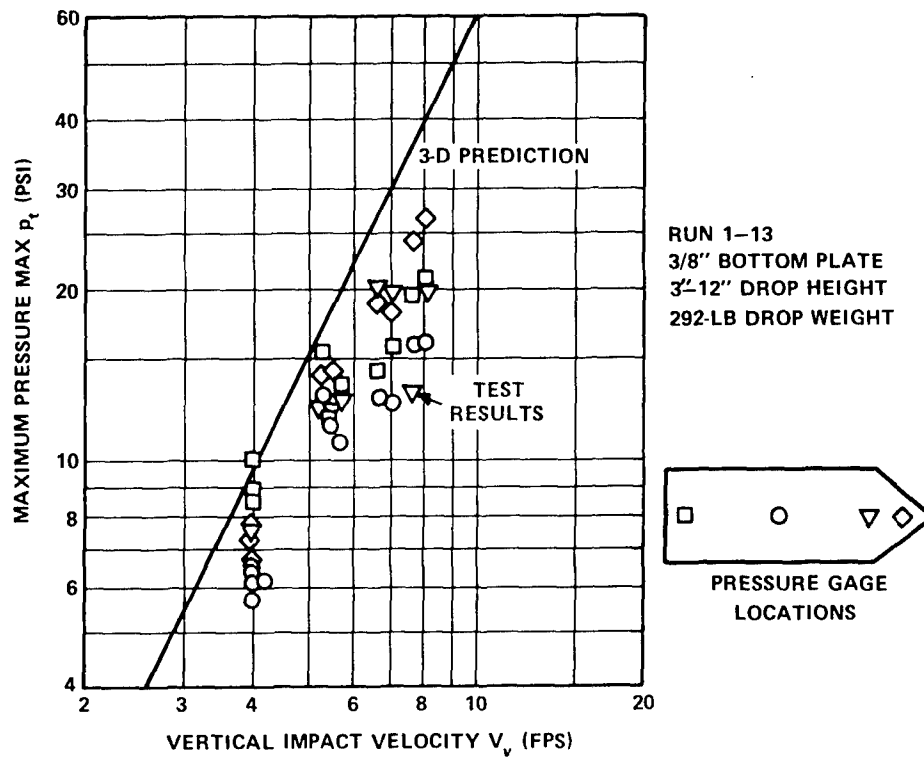


Figure 5a -- Maximum Impact Pressure

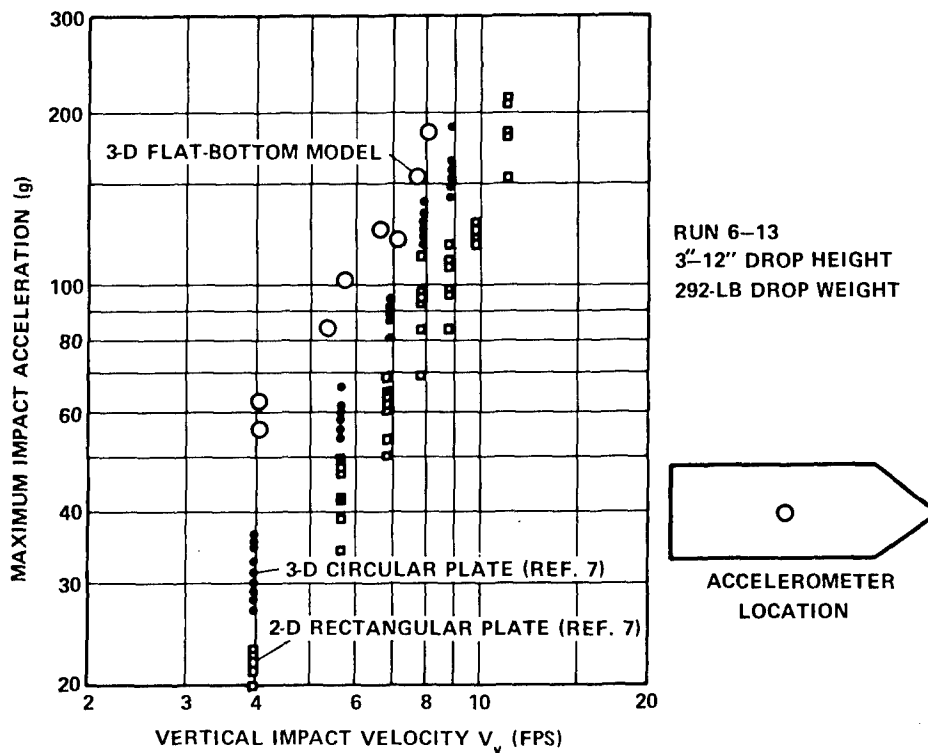


Figure 5b -- Maximum Impact Accelerations

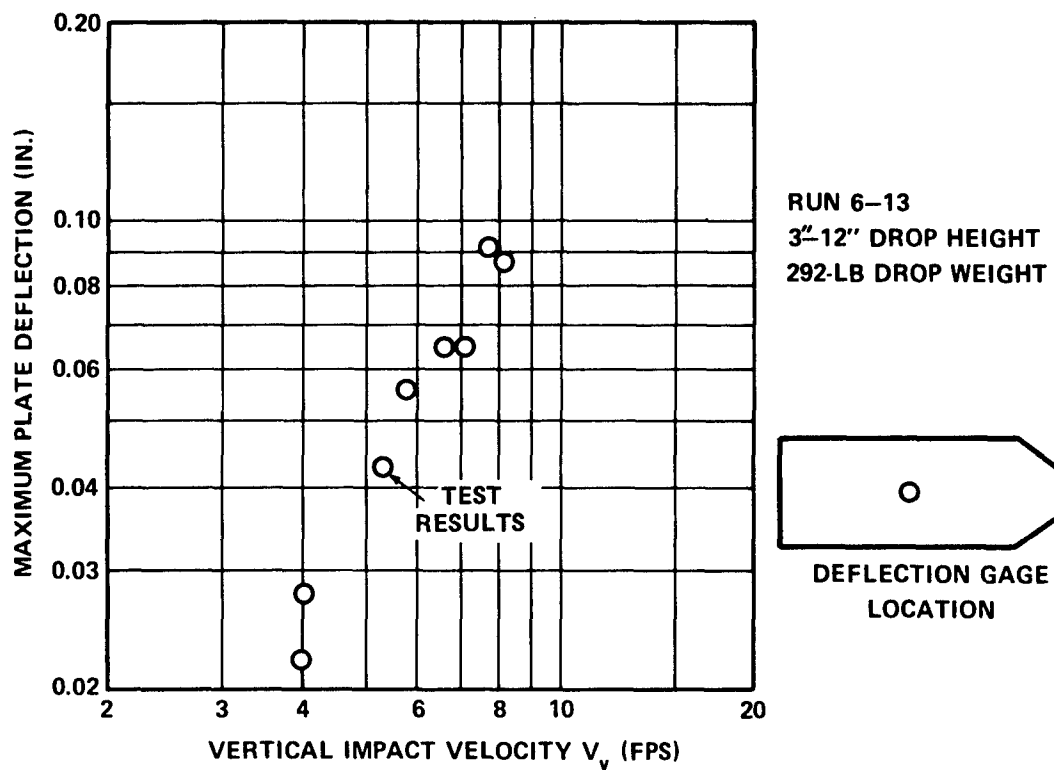


Figure 5c - Maximum Plate Deflection

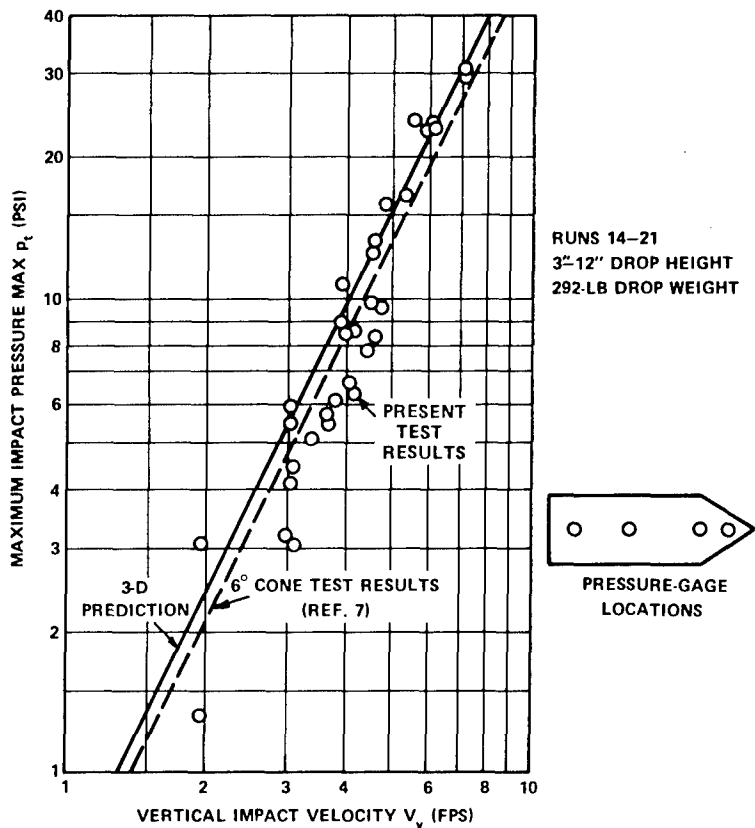


Figure 6 — Maximum Impact Pressure during Calm Water Impact of Three-Dimensional Flat-Bottom Model with 6-Degree Trim and Zero Horizontal Velocity

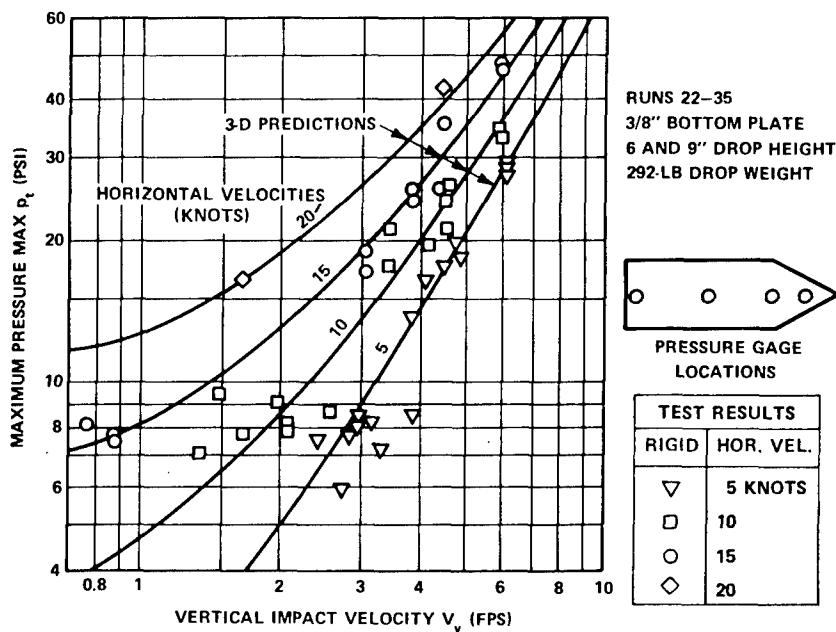


Figure 7 — Maximum Impact Pressure during Calm Water Impact of Three-Dimensional Flat-Bottom Model with 6-Degree Trim and Various Horizontal Velocities

Figure 8 – Calm Water Impact of Three-Dimensional Flat-Bottom Model with Zero Trim and Various Horizontal Velocities

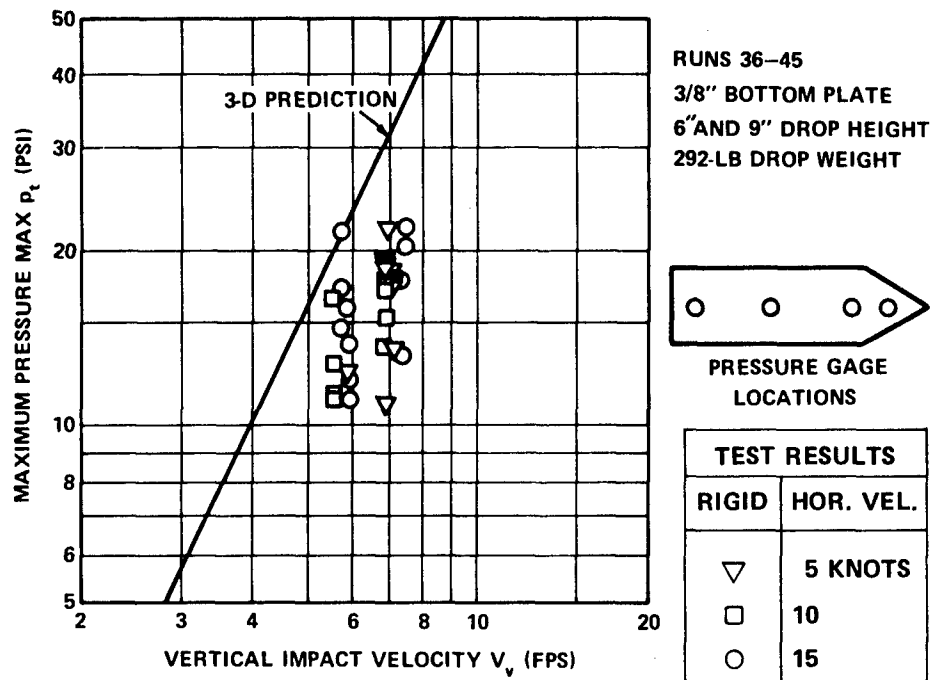


Figure 8a – Maximum Impact Pressure

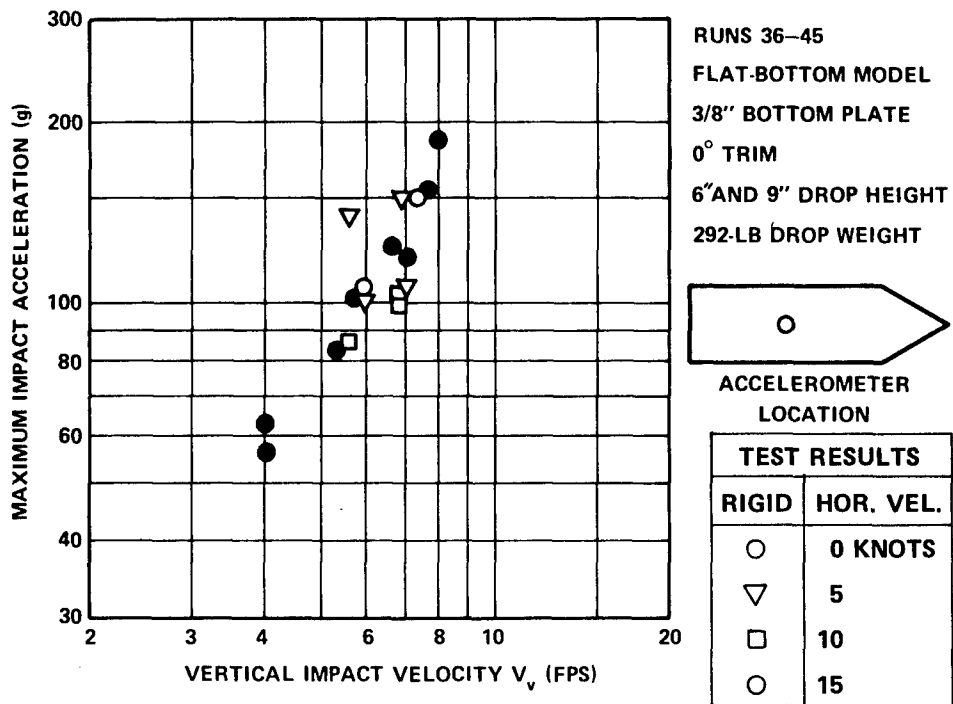
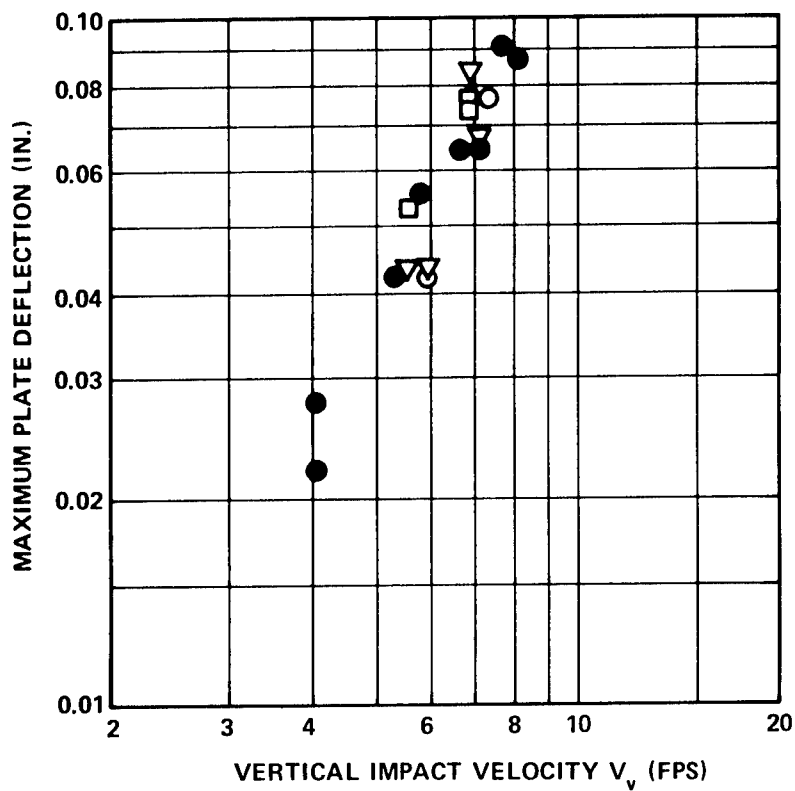


Figure 8b – Maximum Impact Acceleration



RUNS 36-45
 FLAT-BOTTOM MODEL
 3/8" BOTTOM PLATE
 6" AND 9" DROP HEIGHT
 292-LB DROP WEIGHT

Figure 8c - Maximum Plate Deflection

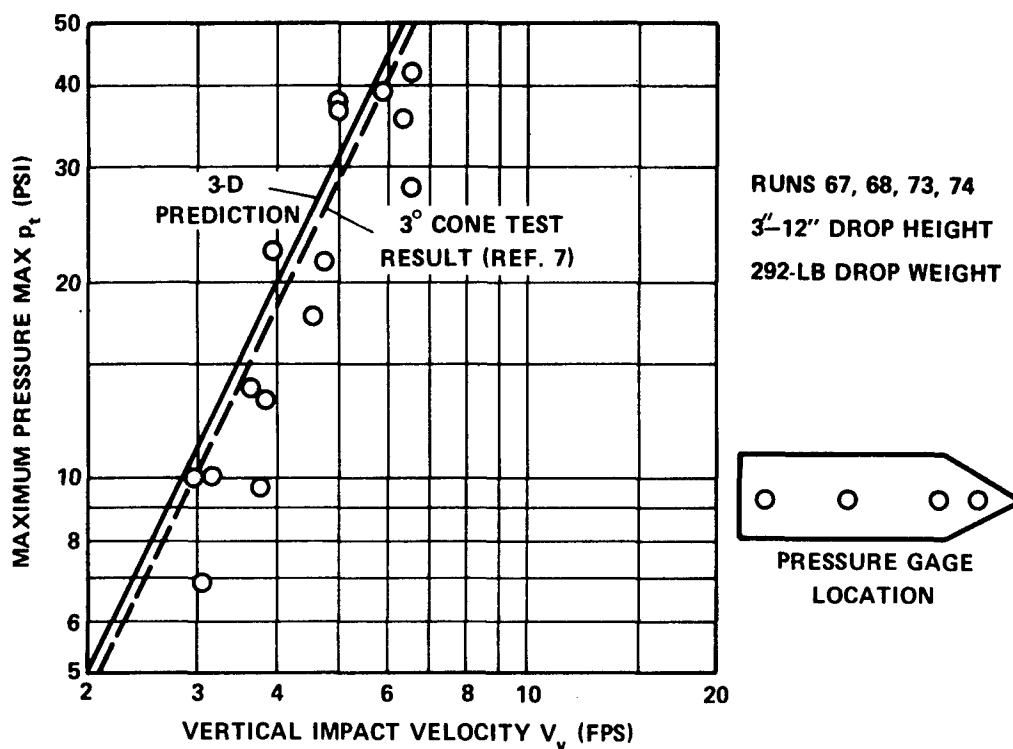


Figure 9 – Maximum Impact Pressure during Calm Water Impact of Three-Dimensional Flat-Bottom Model with -3-Degree Trim and Zero Horizontal Velocity

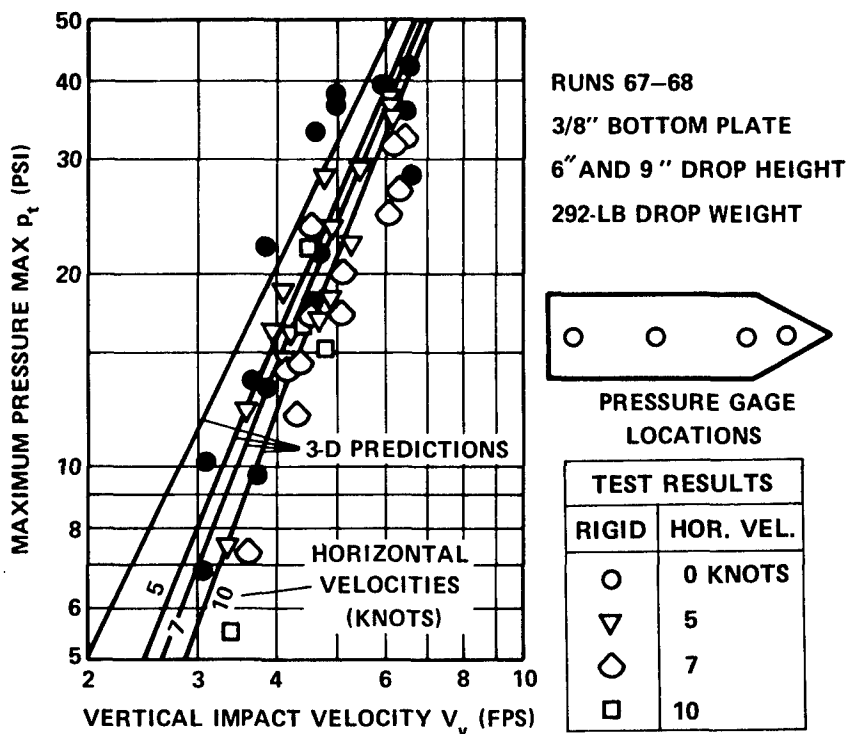


Figure 10 – Maximum Impact Pressure during Calm Water Impact of Three-Dimensional Flat-Bottom Model with -3-Degree Trim and Various Horizontal Velocities

Figure 11 – Effect of Added Weight on Calm Water Impact of Three-Dimensional Flat-Bottom Model with Zero Trim and Zero Horizontal Velocity

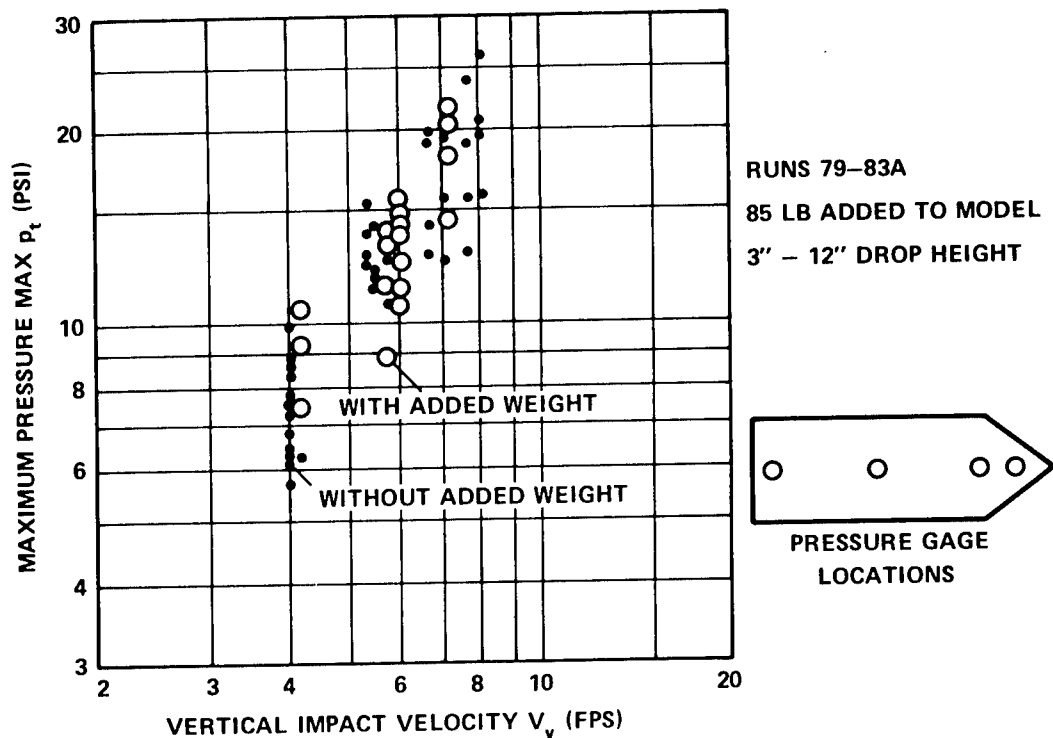


Figure 11a – Maximum Impact Pressure

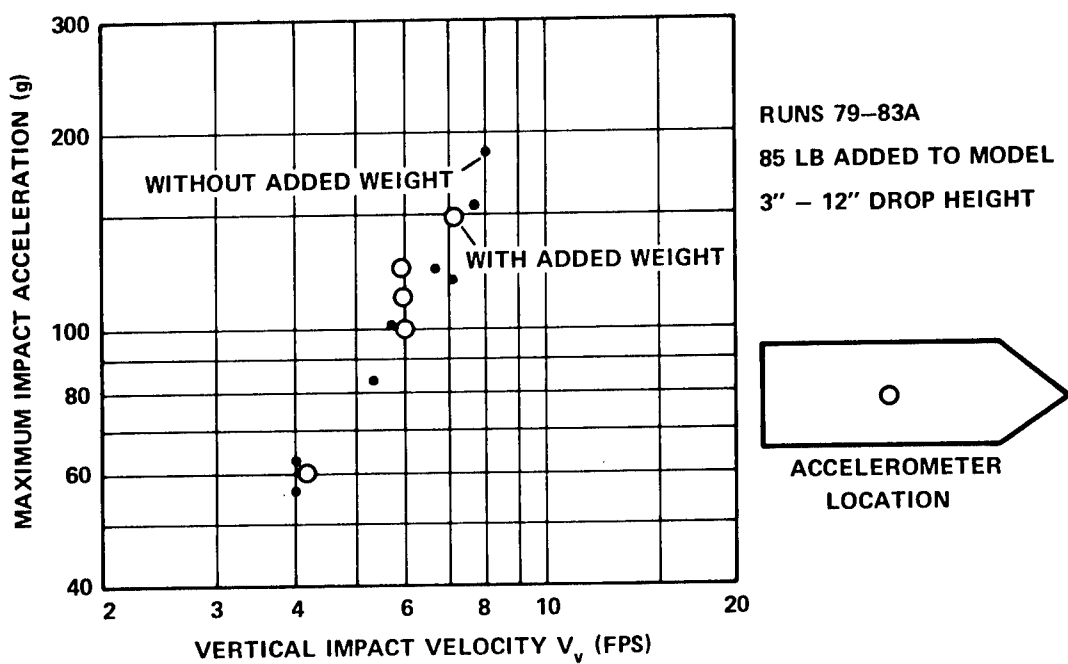


Figure 11b – Maximum Impact Acceleration

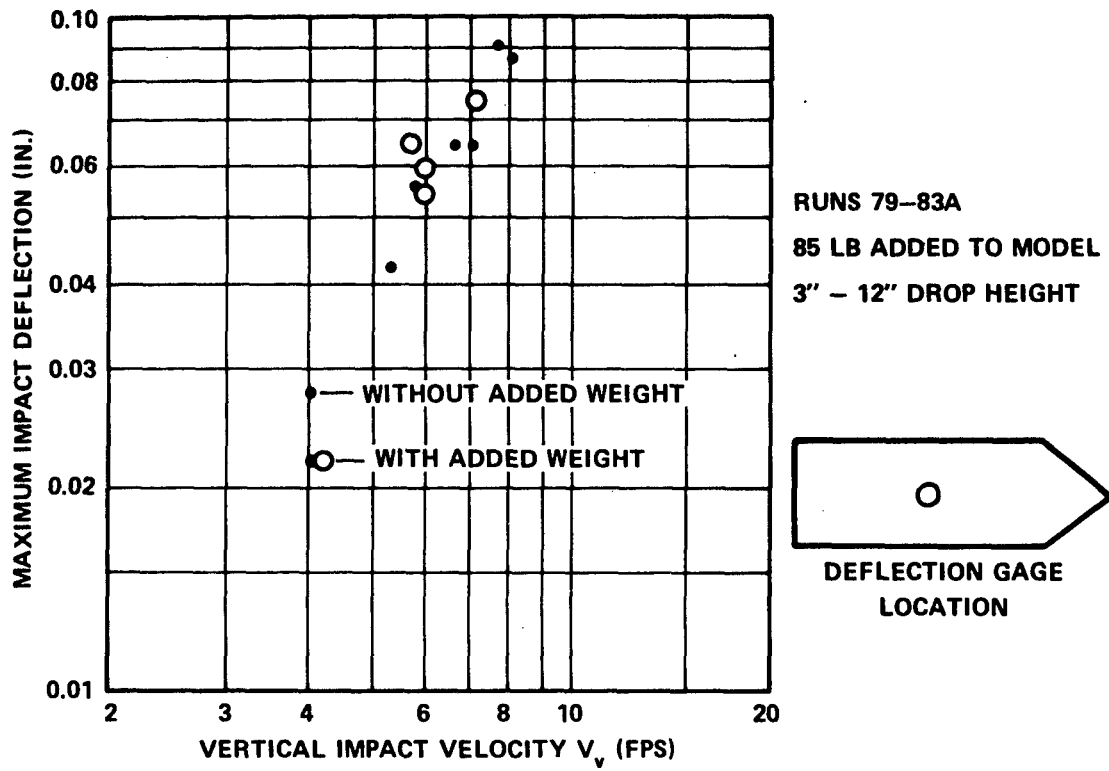


Figure 11c - Maximum Plate Deflection

Figure 12 – Effect of Added Weight on Calm Water Impact of Three-Dimensional Flat-Bottom Model with Zero Trim and 10-Knot Horizontal Velocity

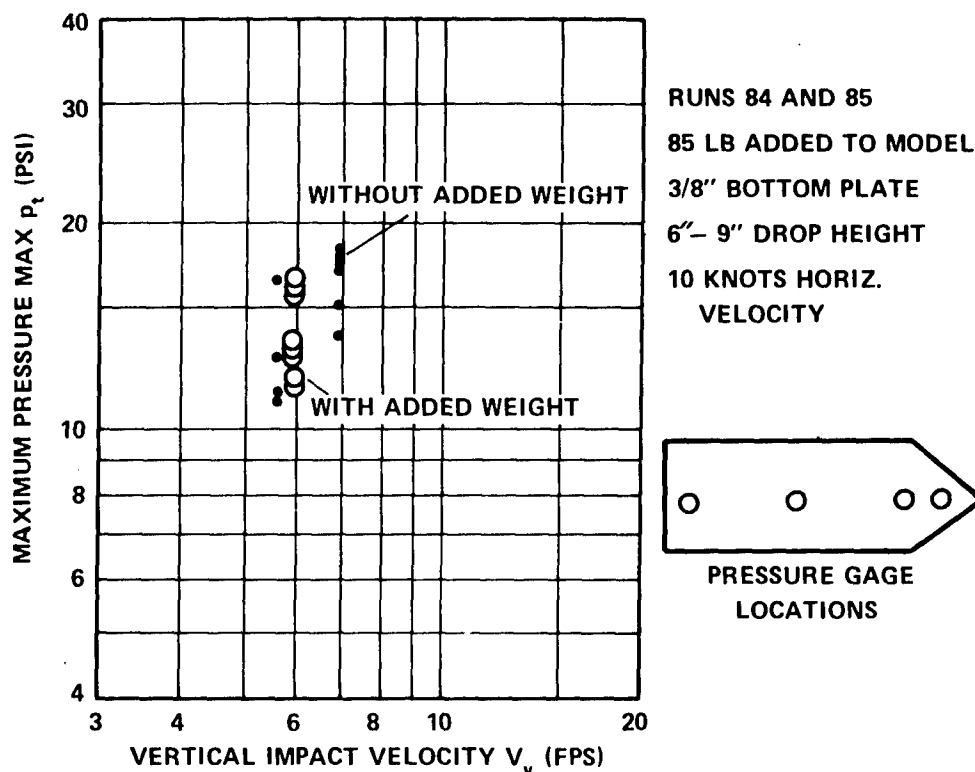


Figure 12a – Maximum Impact Pressure

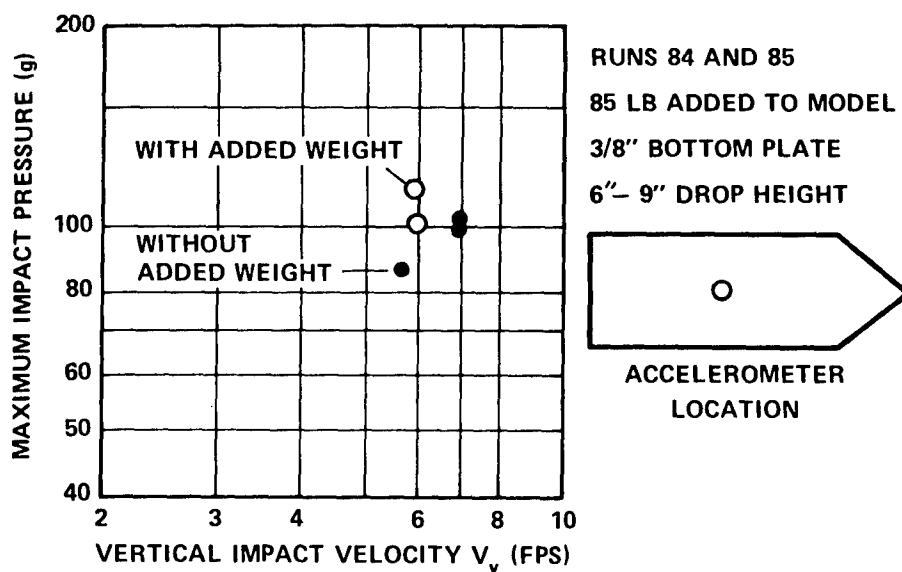


Figure 12b – Maximum Impact Acceleration

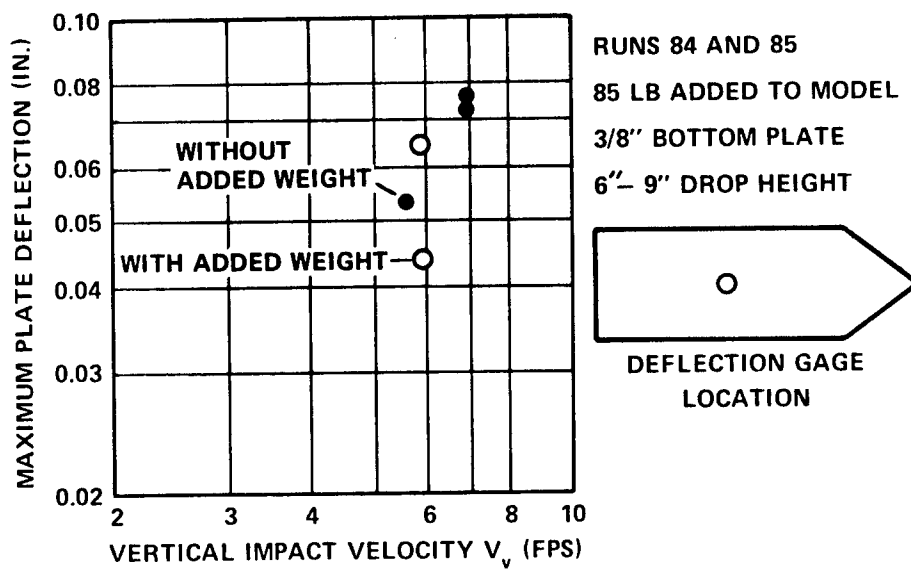


Figure 12c - Maximum Plate Deflection

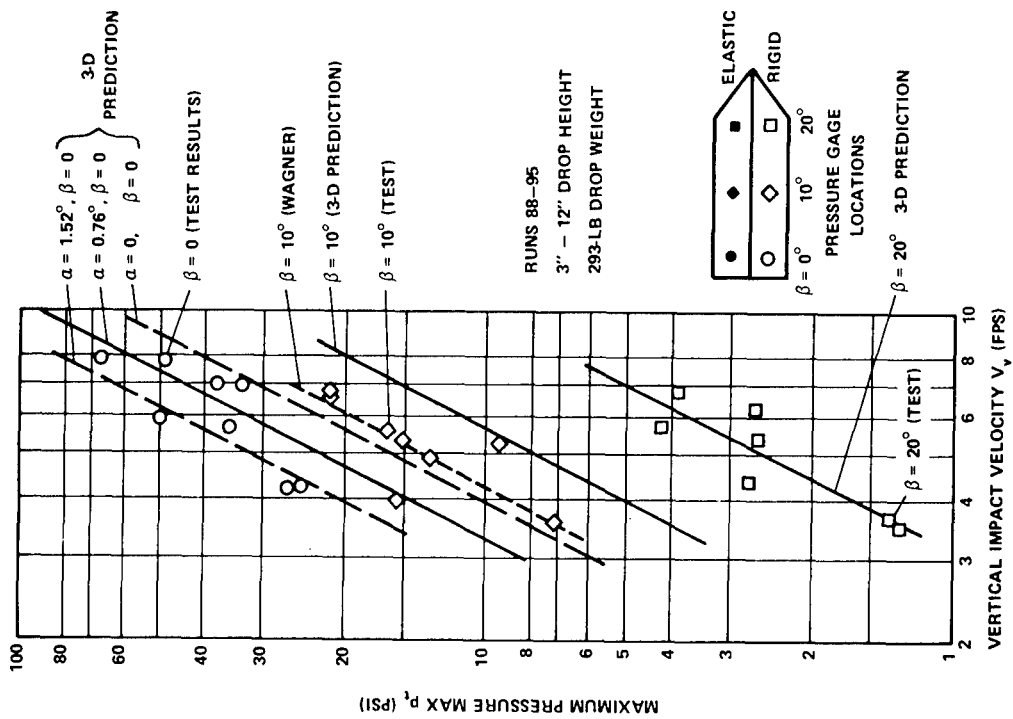


Figure 13 — Maximum Impact Pressure during Calm Water Impact of Three-Dimensional Varying-Deadrise Angle Model with Zero Trim and Zero Horizontal Velocity

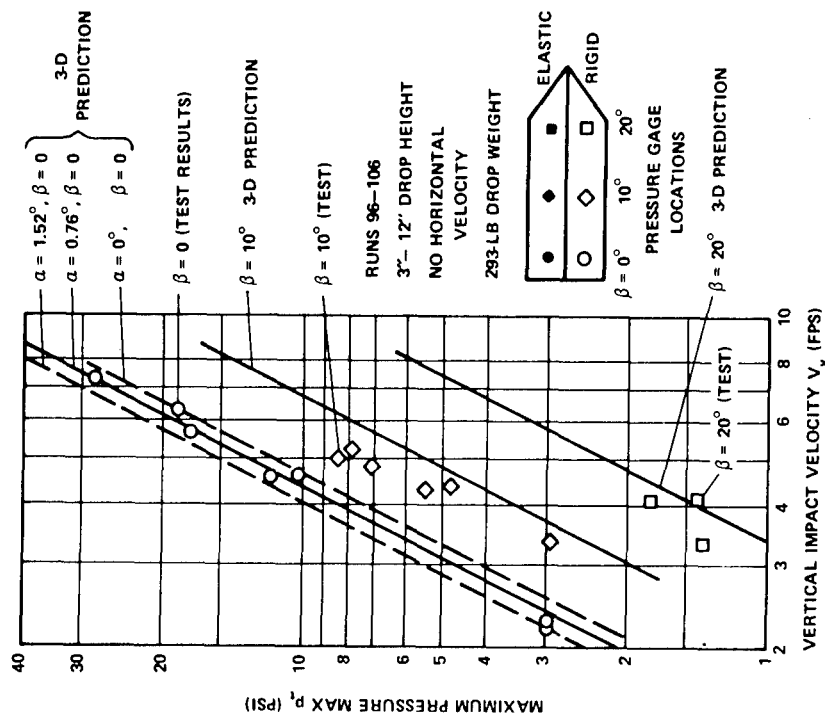


Figure 14 — Maximum Impact Pressure during Calm Water Impact of Three-Dimensional Varying-Deadrise Angle Model with 6-Degree Trim and Zero Horizontal Velocity

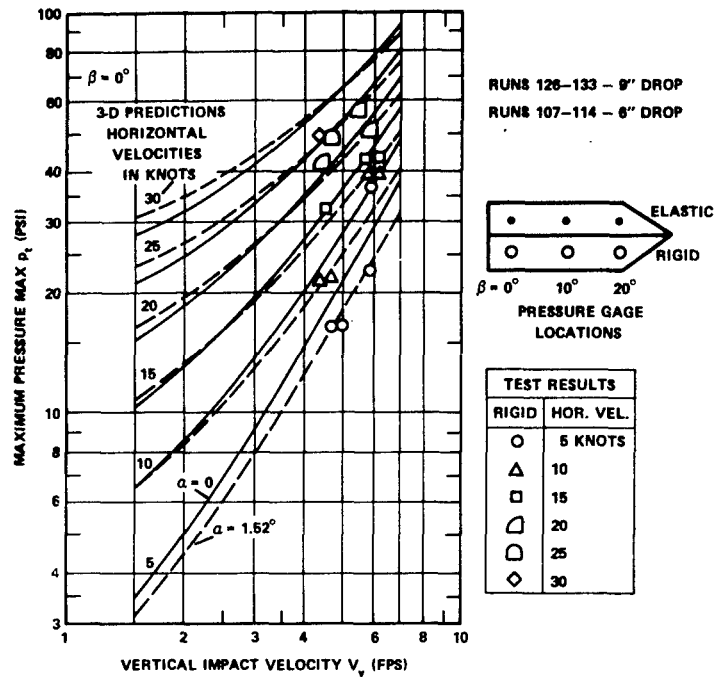


Figure 15a - At $\beta = 0$ Degrees

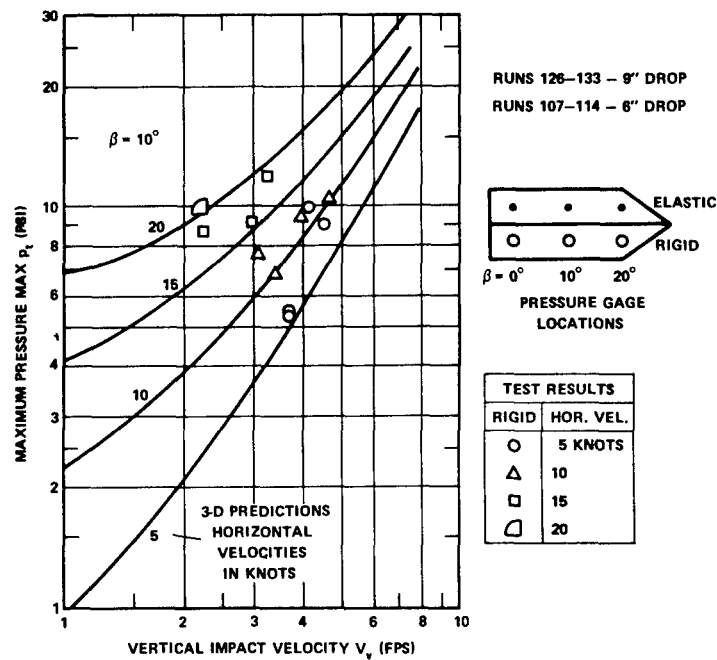


Figure 15b - At $\beta = 10$ Degrees

Figure 15 - Maximum Impact Pressure during Calm Water Impact of Three-Dimensional Varying-Deadrise Angle Model with 6-Degree Trim and Various Horizontal Velocities

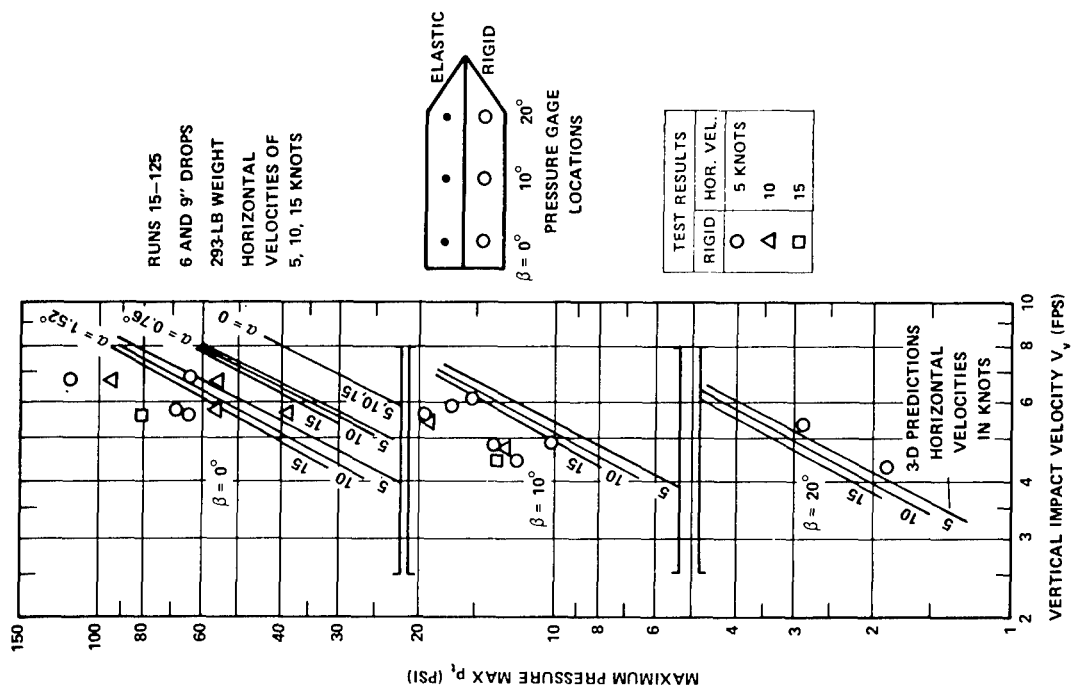


Figure 16 — Maximum Impact Pressure during Calm Water Impact of Three-Dimensional Varying-Deadrise Angle Model with Zero Trim and Various Horizontal Velocities

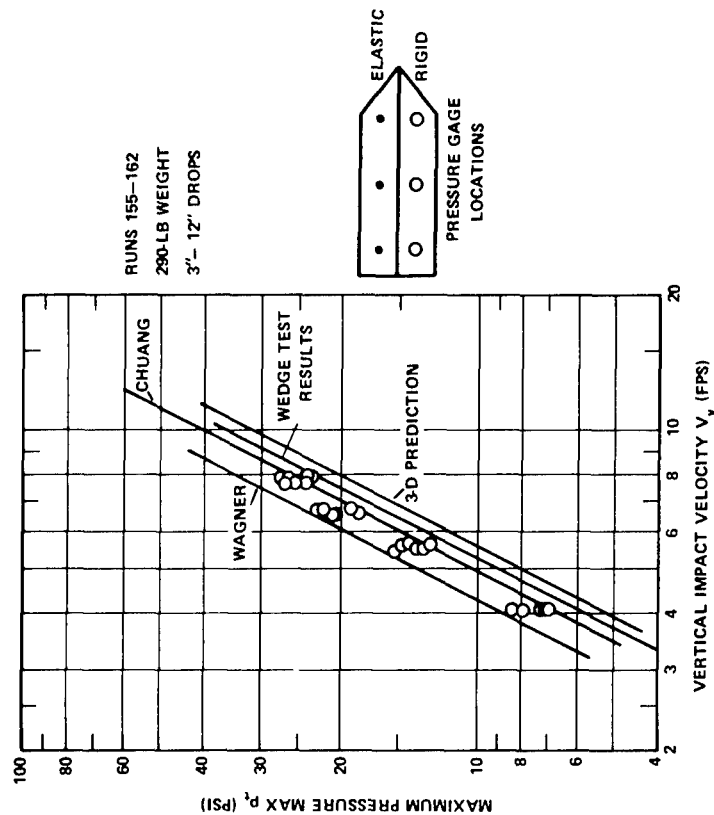


Figure 17 — Maximum Impact Pressure during Calm Water Impact of Three-Dimensional 10-Degree Model with Zero Trim and Zero Horizontal Velocity

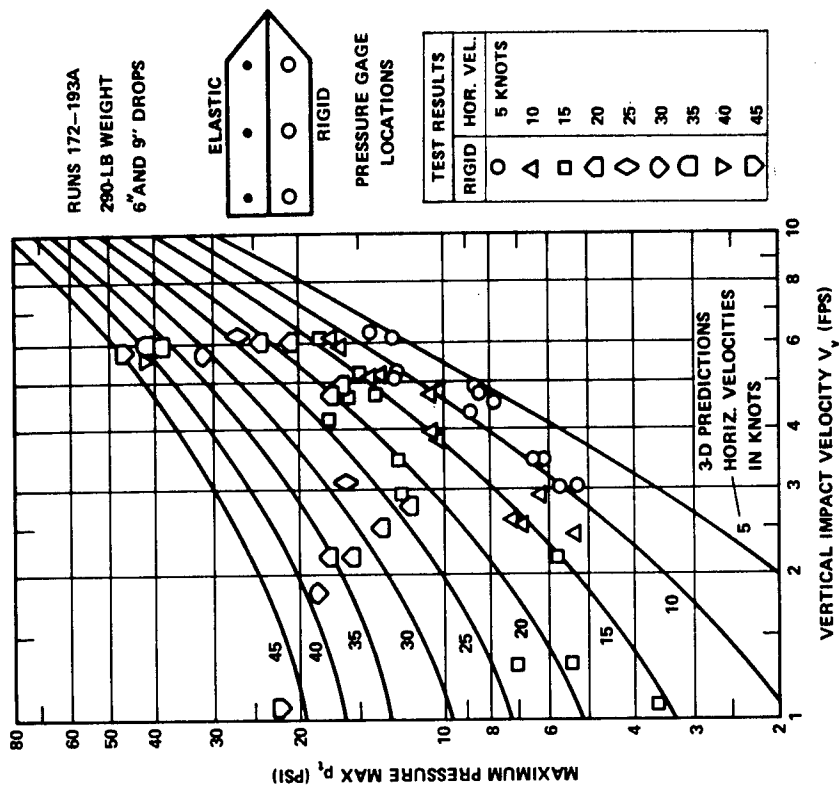


Figure 19 - Maximum Impact Pressure during Calm Water
Impact of Three-Dimensional 10-Degree Model with
6-Degree Trim and Various Horizontal Velocities

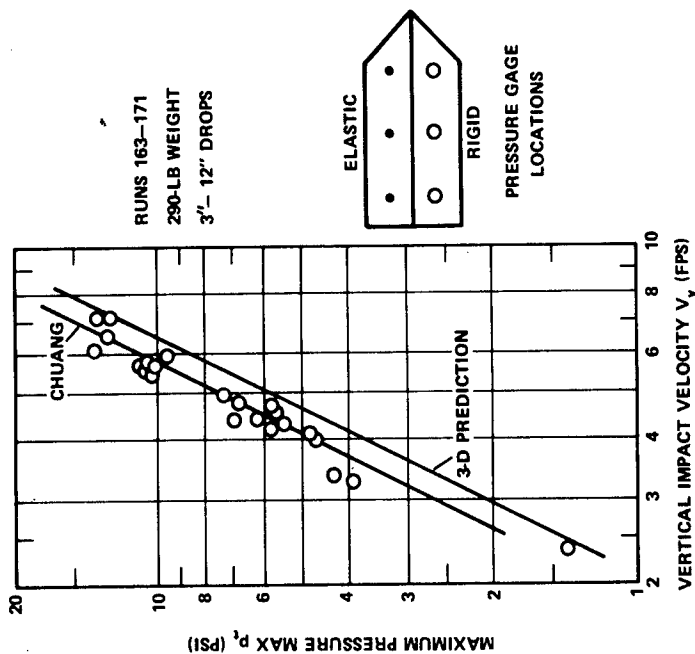


Figure 18 - Maximum Impact Pressure during Calm Water
Impact of Three-Dimensional 10-Degree Model with
6-Degree Trim and Zero Horizontal Velocity

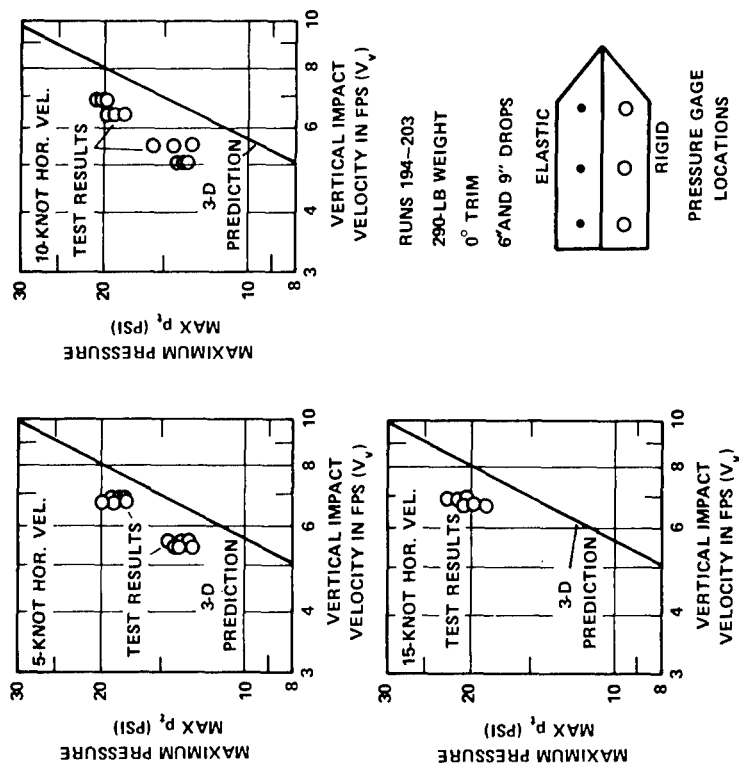


Figure 20 — Maximum Impact Pressure during Calm Water Impact of Three-Dimensional 10-Degree Model with Zero Trim and Various Horizontal Velocities

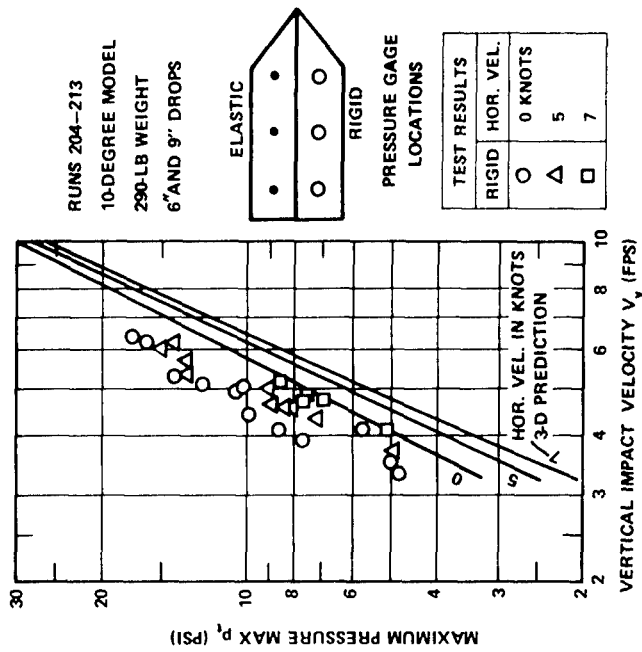


Figure 21 — Maximum Impact Pressure during Calm Water Impact of Three-Dimensional 10-Degree Model with ~3 Degree Trim and Various Horizontal Velocities

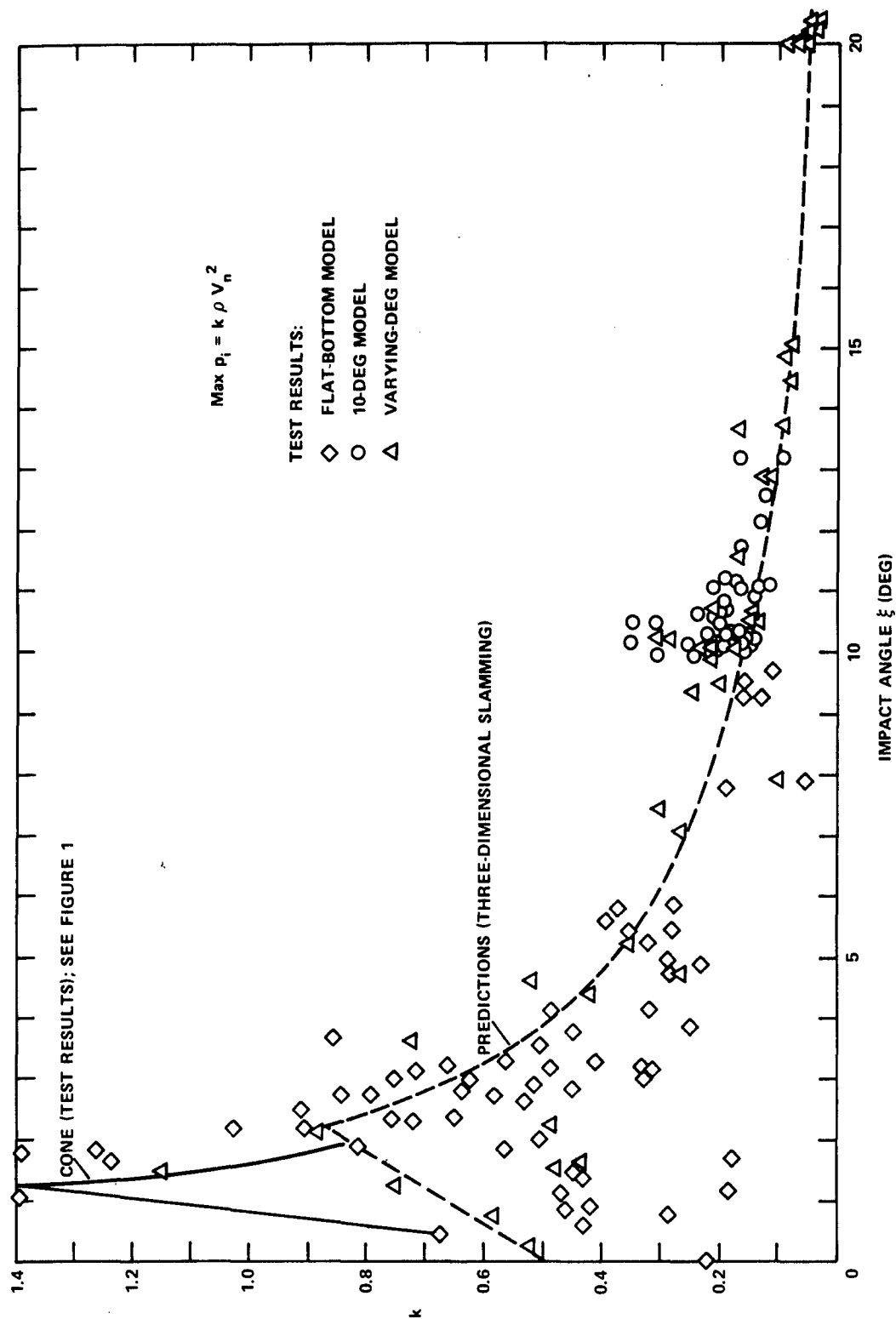


Figure 22 -- Comparison of Predicted and Experimental Results for Various Models in Waves

Figure 23 — Elasticity Effect on Maximum Impact Pressure of the Three-Dimensional Varying-Deadrise Angle Model

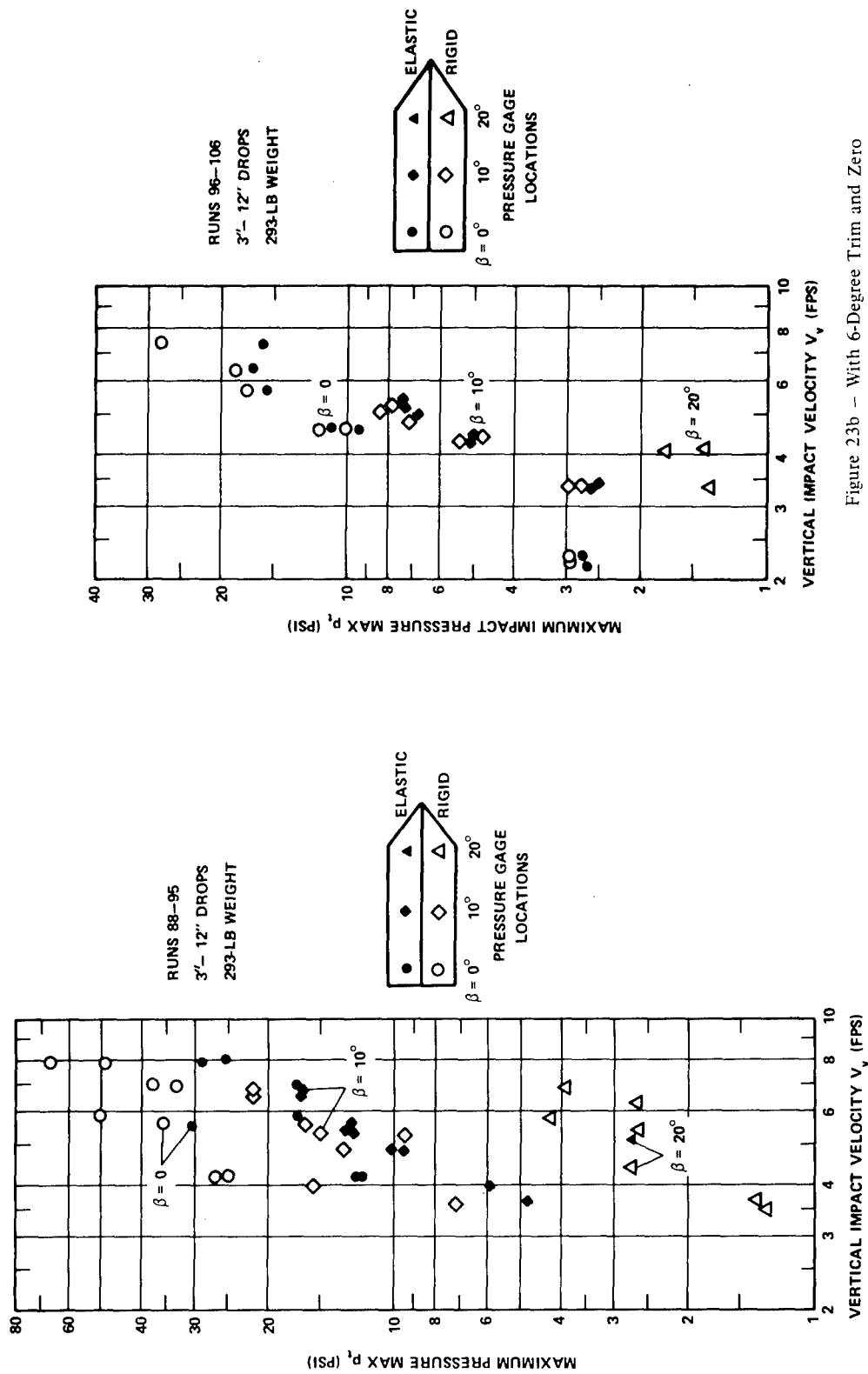


Figure 23a — With Zero Trim and Zero Horizontal Velocity

Figure 23b — With 6-Degree Trim and Zero Horizontal Velocity

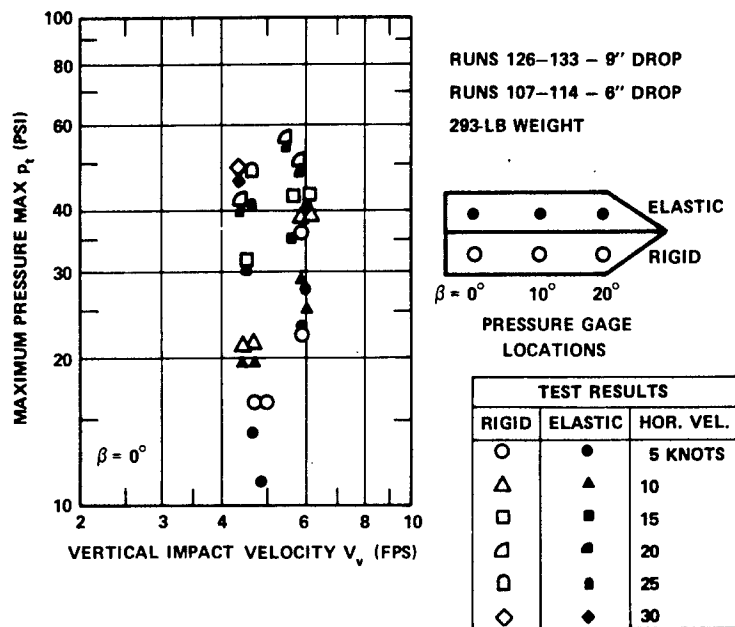


Figure 23c - With 6-Degree Trim and Various
 Horizontal Velocities at $\beta = 0$ Degrees

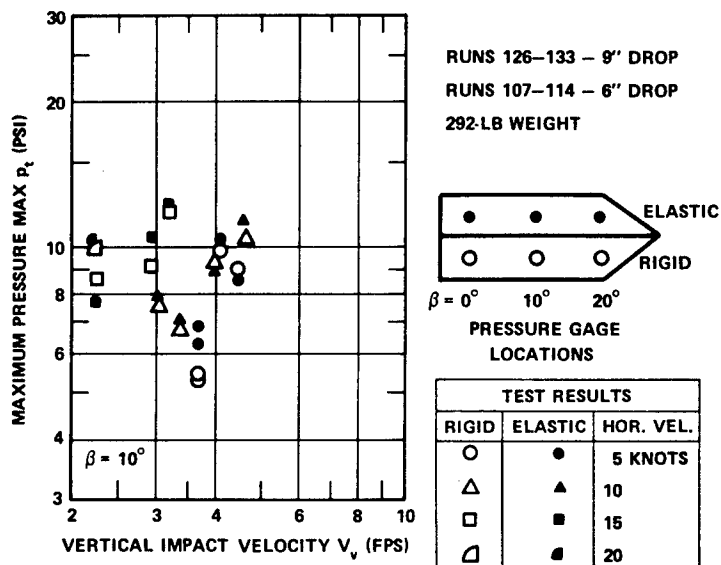


Figure 23d - With 6-Degree Trim and Various
 Horizontal Velocities at $\beta = 10$ Degrees

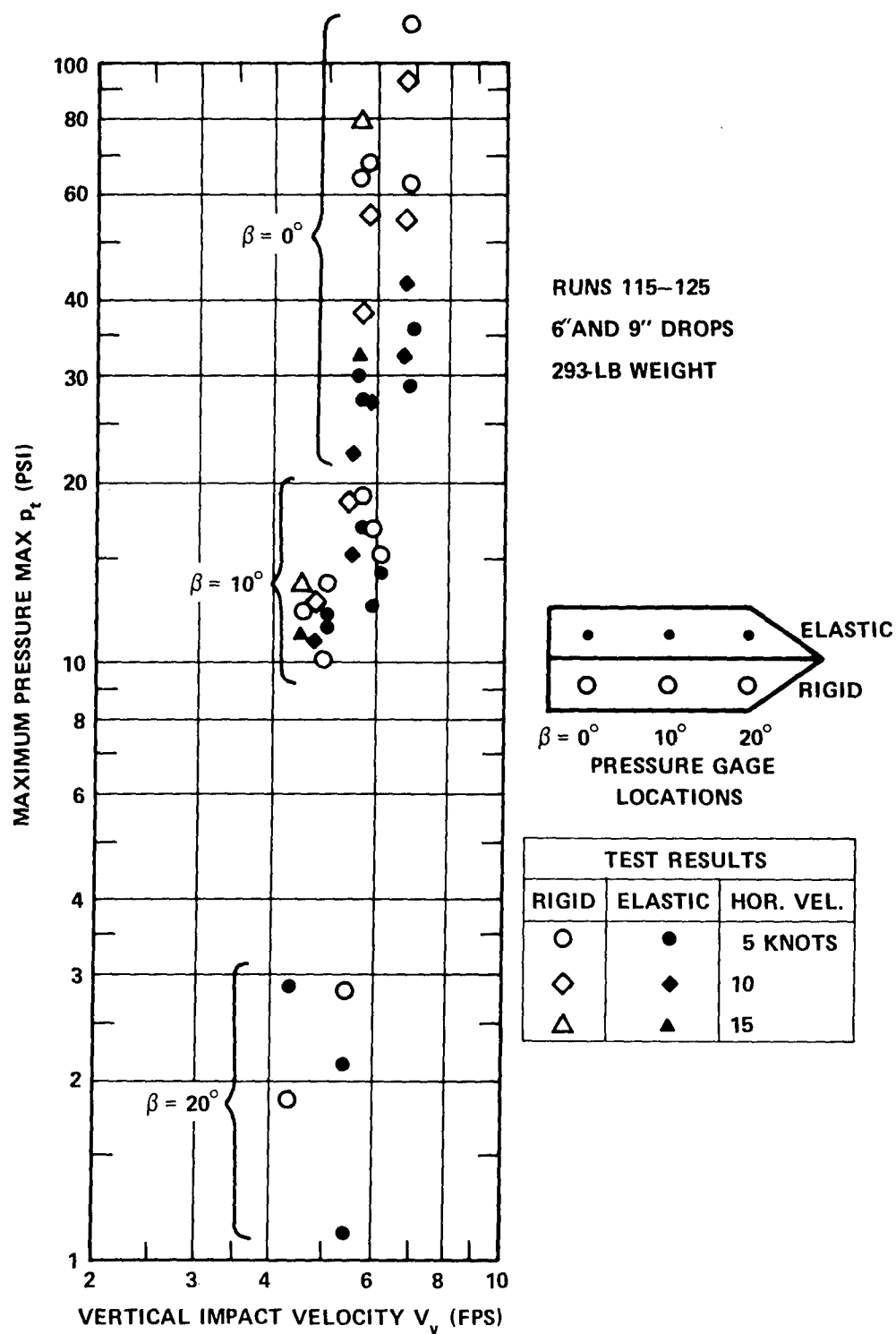


Figure 23e - With Zero Trim and Various
Horizontal Velocities

Figure 24 – Elasticity Effect on Maximum Impact Pressure of the Three-Dimensional 10-Degree Model

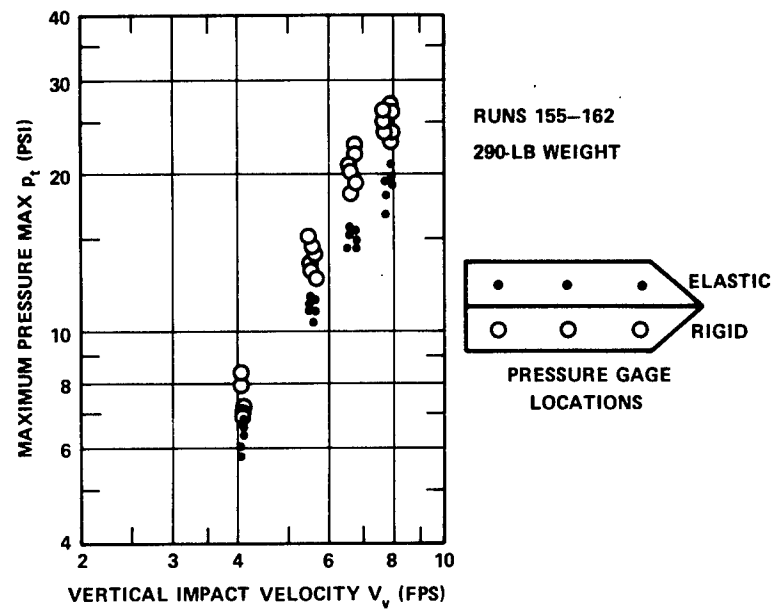


Figure 24a – Zero Trim and Zero
Horizontal Velocity

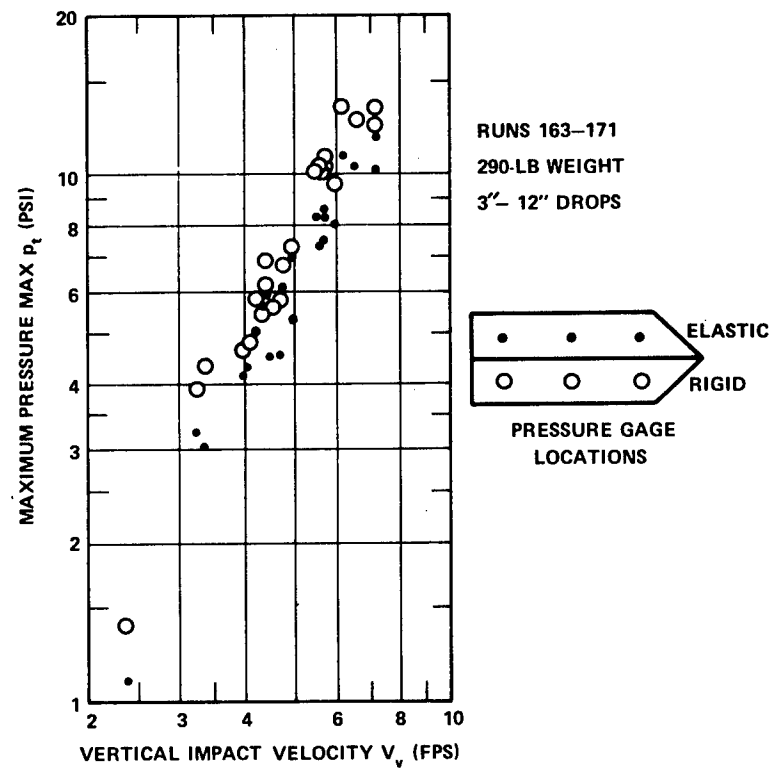


Figure 24b – With 6-Degree Trim and Zero
Horizontal Velocity

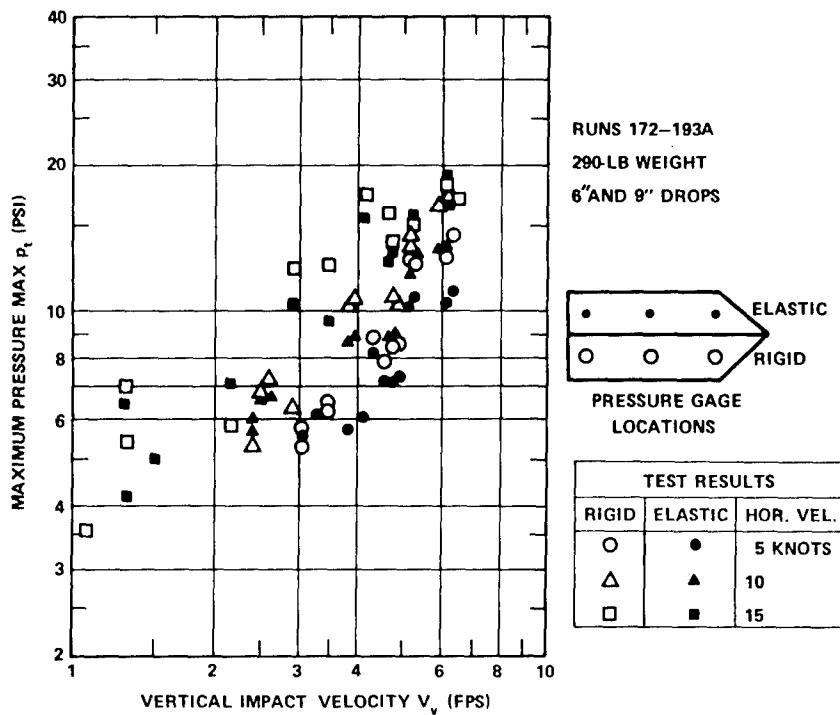


Figure 24c - With 6-Degree Trim and Horizontal Velocities of 5, 10, and 15 Knots

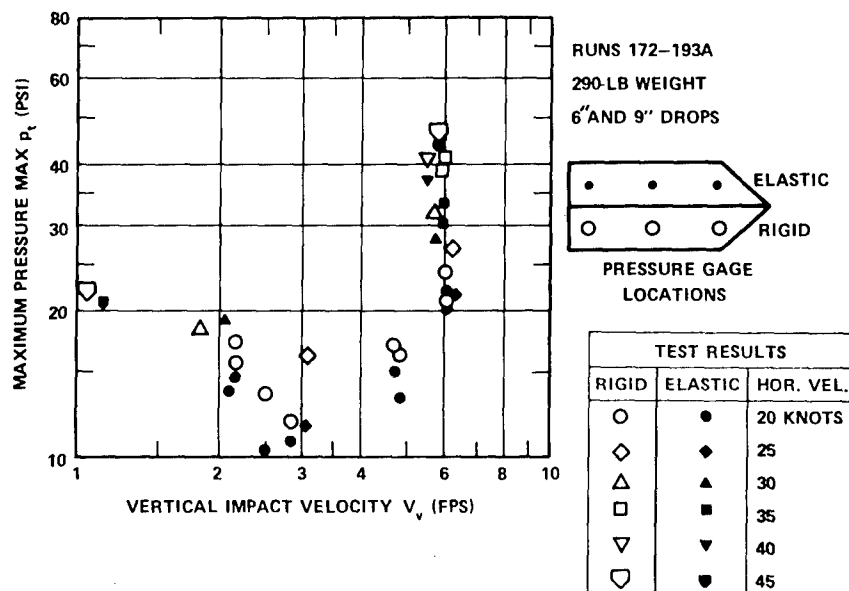


Figure 24d - With 6-Degree Trim and Horizontal Velocities from 20-45 Knots

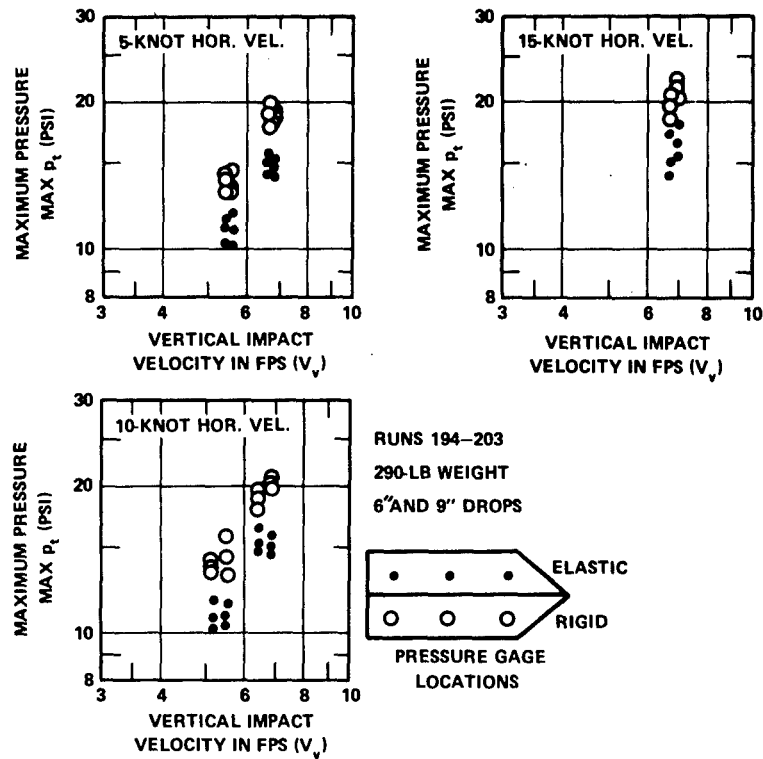


Figure 24e - With Zero Trim and Various Horizontal Velocities

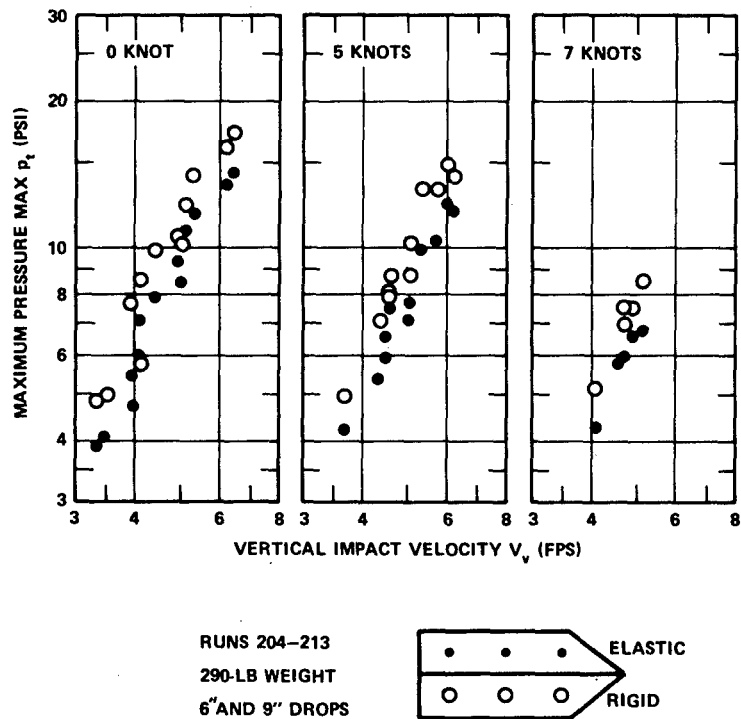


Figure 24f - With -3 Degree Trim and Various Horizontal Velocities

TABLE 1 - COMPARISON OF EXPERIMENTAL AND PREDICTED SLAMMING PRESSURES FOR FLAT-BOTTOM MODEL IN WAVES

Run Number	Gage Number	β deg	τ deg	α deg	ξ deg	V_h knots	V_v fps	V_n fps	V_t fps	L_w ft	h in.	θ deg	y percent L_w	p_p psi	p_i psi	p_t , psi		k
																Calc	Exp	
46	P5	0	0	0	3.05	0	2.53	3.178	12.10	29.4	8.5	3.05	0.126	-0.99	12.56	11.57	6.3	0.322
	P7				2.01		2.74	3.167	12.15			2.01	0.174	-1.00	15.64	14.64	12.4	0.637
	P9				0.22		3.18	3.227	12.24			0.22	0.242	-1.01	7.16	6.15	9.8	0.485
	P10				0.23		3.18	3.132	12.27			-0.23	0.258	1.01	6.78	7.79	6.15	0.323
47	P5	0	0	0	1.99	0	2.87	3.304	12.48	31.0	6.75	1.99	0.146	-1.05	16.88	15.83	17.1	0.807
	P7				0.99		3.79	4.007	12.52			0.99	0.201	-1.06	15.96	14.90	13.0	0.417
	P10				1.01		2.32	2.098	12.62			-1.01	0.3	1.07	4.42	5.49	11.9	1.394
	P5	0	0	0	4.08	0	2.37	3.236	12.05	29.4	8.0	4.08	0.005	-0.98	9.54	8.56	6.49	0.319
48	P7				3.85		2.96	3.776	12.03			3.85	0.054	-0.97	13.84	12.87	12.3	0.445
	P9				2.97		3.95	4.580	12.03			2.97	0.120	-0.98	26.74	25.77	25.3	0.522
	P10				2.66		2.66	4.513	12.06			2.66	0.137	-0.98	29.03	28.05	31.5	0.797
	P5	0	0	0	0.42	5	3.61	3.70	12.39	30.2	8.75	0.42	-0.235	-1.04	10.38	9.34	18.1	0.682
49	P7				1.83		4.95	5.34	12.26			1.83	-0.191	-1.01	41.27	40.26	77.0	1.392
	P9				3.29		7.21	7.91	11.99			3.29	-0.114	-0.97	71.93	70.96	49.0	0.404
	P5	0	0	0	3.84	5	2.68	3.51	12.27	30.5	7.81	3.84	0.005	-1.02	11.99	10.97	6.0	0.251
	P7				3.65		3.35	4.14	12.24			3.65	0.05	-1.01	17.60	16.59	28.6	0.860
50	P9				2.98		4.21	4.85	12.25			2.98	0.109	-1.01	29.98	28.97	34.6	0.758
	P10				2.70		4.31	4.89	12.26			2.70	0.126	-1.01	33.55	32.54	27.0	0.582
	P5	0	0	0	3.56	10	5.83	5.04	12.84	30.6	7.30	-3.56	-0.483	1.11	26.88	27.99	25.0	0.507
	P7				3.17		5.12	4.42	12.77			-3.17	-0.423	1.10	23.39	24.49	24.7	0.552
51	P9				2.62		4.40	3.82	12.69			-2.62	-0.381	1.09	21.06	22.15	15.0	0.530
	P10				0.85		4.40	4.21	12.57			-0.85	-0.288	1.06	16.54	17.60	9.8	0.285
	P5	0	0	0	2.86	0	2.53	3.027	9.91	19.75	7.37	2.86	-0.165	-0.66	12.17	11.51	8.0	0.450
	P7				4.79		3.52	4.347	9.72			4.79	-0.087	-0.64	14.47	13.83	10.3	0.281
52	P9				5.59		4.51	5.467	9.56			5.59	0.008	-0.62	19.41	18.79	23.1	0.398
	P10				5.47		4.51	5.447	9.57			5.47	0.034	-0.62	19.72	19.10	15.8	0.274

TABLE I (Continued)

Run Number	Gage Number	β deg	τ deg	α deg	ξ deg	V_h knots	V_v fps	V_n fps	V_t fps	L_w ft	h in.	θ deg	y percent L_w	P_p psi	P_i psi	P_t , psi		k
																Calc	Exp	
53	P5	0	0	0	4.08	0	2.41	3.144	10.21	21.2	7.63	4.08	0.114	-0.70	9.01	8.31	9.34	0.487
	P7				1.89		3.18	3.522	10.30			1.89	0.193	-0.71	18.44	17.73	13.4	0.557
	P9				1.57		3.95	3.663	10.51			-1.57	0.297	0.74	17.38	18.12	31.9	1.226
	P10				2.42		3.30	2.858	10.54			2.42	0.324	0.75	12.68	13.43	14.3	0.902
54	P5	0	0	0	4.89	5	2.42	3.256	9.66	19.2	7.75	4.89	-0.100	-0.63	7.94	7.31	4.7	0.229
	P7				5.88		3.74	4.735	9.47			5.88	-0.038	-0.60	13.78	13.18	12.0	0.276
	P9				5.74		4.27	5.239	9.43			5.74	0.052	-0.60	17.33	16.73	20.0	0.376
	P10				5.38		4.60	5.508	9.43			5.38	0.076	-0.60	20.53	19.93	20.4	0.347
55	P5	0	0	0	1.03	10	3.19	3.369	9.90	19.4	7.13	1.03	0.22	-0.66	11.52	10.86	4.0	0.182
	P7				3.18		4.51	5.056	9.69			3.18	-0.152	-0.63	30.38	29.75	15.7	0.317
	P9				4.95		5.61	6.448	9.43			4.95	-0.073	-0.60	30.74	30.14	23.1	0.286
	P10				5.21		5.48	6.361	9.42			5.21	-0.053	-0.60	28.33	27.73	25.2	0.321
56	P5	0	6	0	7.88	0	3.83	3.418	12.62	30.6	7.63	-1.88	-0.666	1.07	5.10	6.18	1.3	0.057
	P7				9.34		3.62	2.885	12.69			-3.34	-0.574	1.08	2.88	3.96	2.6	0.161
	P9				9.59		4.16	3.370	12.74			-3.59	-0.454	1.09	3.78	4.87	2.4	0.109
	P10				9.32		4.16	3.429	12.72			-3.32	-0.424	1.09	4.08	5.17	3.0	0.132
57	P5 P7	0 	6 	0 	2.87 2.33	0 	4.81 3.62	5.482 4.407	12.14 12.16	30.2 	7.50 	3.13 3.67	-0.091 -0.028	0.99 1.00	39.74 31.15	40.74 32.15	29.7 27.2	0.509 0.722
58	P5 P7	0 	6 	0 	9.45 7.77	5 	5.39 4.83	5.510 5.322	12.76 12.58	29.7 	7.63 	-3.45 -1.77	-0.427 -0.326	1.10 1.07	10.32 12.60	11.42 13.67	9.34 10.7	0.159 0.195
59	P5 P7 P9 P10	0 	6 	0 	3.26 2.27 2.13 2.30	10 	5.44 4.52 2.56 2.23	7.792 7.084 5.158 4.791	12.26 12.18 12.29 12.33	30.25 	8.0 	2.74 3.73 3.87 3.70	-0.128 -0.055 0.035 0.059	1.01 1.00 1.02 1.02	70.49 82.59 43.63 37.22	71.51 83.59 44.64 38.25	67.0 64.0 46.5 33.7	0.569 0.657 0.901 0.757
61	P5 P7 P9 P10	0 	6 	0 	1.48 0.65 2.16 3.11	5 	5.17 3.33 2.96 2.31	6.840 5.148 4.517 3.702	9.77 9.84 10.00 10.10	20.3 	7.25 	4.53 5.35 3.84 2.89	-0.090 0.007 0.123 0.159	0.64 0.65 0.67 0.69	58.06 22.41 33.89 16.69	58.70 23.06 34.56 17.38	40.0 22.3 41.0 18.9	0.441 0.434 1.036 0.711

TABLE 1 (Continued)

Run Number	Gage Number	β deg	τ deg	α deg	ξ deg	V_h knots	V_v fps	V_n fps	V_t fps	L_w ft	h in.	θ deg	y percent L_w	p_p psi	p_i psi	p_t , psi		k
																Calc	Exp	
64	P5	0	6	0	1.66	10	0.00	3.415	12.22	30.0	16.0 *	7.66	-0.047	-1.01	15.71	14.70	4.0	0.177
	P7				2.00			3.487	12.20			8.00	0	-1.00	18.91	17.91	12.0	0.509
	P9				1.48			3.377	12.23			7.48	0.058	-1.01	14.21	13.20	9.6	0.434
	P10				1.17			3.311	12.25			7.17	0.073	-1.01	11.87	10.86	10.0	0.470
86	P5	0	0	0	2.74	5	7.02	6.409	12.94	31.2	8.0	-2.74	-0.376	1.13	56.85	57.98	67.5	0.847
	P7				1.79		6.47	6.073	12.82			-1.79	-0.327	1.11	52.48	53.59	89.9	1.256
	P9				0		3.83	3.830	12.62			0	-0.250	1.07	9.11	10.18	6.1	0.214
	P10				0.79		3.83	4.004	12.57			0.79	-0.217	-1.06	14.52	13.46	13.4	0.431
*Correction made for flat crest and trough of the wave.																		

TABLE 1 (Continued)

Run Number	Gage Number	β deg	τ deg	α deg	ξ deg	V_h knots	V_v fps	V_n fps	V_t fps	L_w ft	h in.	θ deg	y percent L_w	P_p psi	P_i psi	P_t , psi		k
																Calc	Exp	
53	P5	0	0	0	4.08	0	2.41	3.144	10.21	21.2	7.63	4.08	0.114	-0.70	9.01	8.31	9.34	0.487
	P7				1.89		3.18	3.522	10.30			1.89	0.193	-0.71	18.44	17.73	13.4	0.557
	P9				1.57		3.95	3.663	10.51			-1.57	0.297	0.74	17.38	18.12	31.9	1.226
	P10				2.42		3.30	2.858	10.54			2.42	0.324	0.75	12.68	13.43	14.3	0.902
54	P5	0	0	0	4.89	5	2.42	3.256	9.66	19.2	7.75	4.89	-0.100	-0.63	7.94	7.31	4.7	0.229
	P7				5.88		3.74	4.735	9.47			5.88	-0.038	-0.60	13.78	13.18	12.0	0.276
	P9				5.74		4.27	5.239	9.43			5.74	0.052	-0.60	17.33	16.73	20.0	0.376
	P10				5.38		4.60	5.508	9.43			5.38	0.076	-0.60	20.53	19.93	20.4	0.347
55	P5	0	0	0	1.03	10	3.19	3.369	9.90	19.4	7.13	1.03	0.22	-0.66	11.52	10.86	4.0	0.182
	P7				3.18		4.51	5.056	9.69			3.18	-0.152	-0.63	30.38	29.75	15.7	0.317
	P9				4.95		5.61	6.448	9.43			4.95	-0.073	-0.60	30.74	30.14	23.1	0.286
	P10				5.21		5.48	6.361	9.42			5.21	-0.053	-0.60	28.33	27.73	25.2	0.321
56	P5	0	6	0	7.88	0	3.83	3.418	12.62	30.6	7.63	-1.88	-0.666	1.07	5.10	6.18	1.3	0.057
	P7				9.34		3.62	2.885	12.69			-3.34	-0.574	1.08	2.88	3.96	2.6	0.161
	P9				9.59		4.16	3.370	12.74			-3.59	-0.454	1.09	3.78	4.87	2.4	0.109
	P10				9.32		4.16	3.429	12.72			-3.32	-0.424	1.09	4.08	5.17	3.0	0.132
57	P5 P7	0 0	6 0	0 0	2.87 2.33	0	4.81 3.62	5.482 4.407	12.14 12.16	30.2	7.50	3.13 3.67	-0.091 -0.028	0.99 1.00	39.74 31.15	40.74 32.15	29.7 27.2	0.509 0.722
58	P5 P7	0 0	6 0	0 0	9.45 7.77	5	5.39 4.83	5.510 5.322	12.76 12.58	29.7	7.63	-3.45 -1.77	-0.427 -0.326	1.10 1.07	10.32 12.60	11.42 13.67	9.34 10.7	0.159 0.195
59	P5 P7 P9 P10	0 0 0 0	6 6 6 6	0 0 0 0	3.26 2.27 2.13 2.30	10	5.44 4.52 2.56 2.23	7.792 7.084 5.158 4.791	12.26 12.18 12.29 12.33	30.25	8.0	2.74 3.73 3.87 3.70	-0.128 -0.055 0.035 0.059	1.01 1.00 1.02 1.02	70.49 82.59 43.63 37.22	71.51 83.59 44.64 38.25	67.0 64.0 46.5 33.7	0.569 0.657 0.901 0.757
61	P5 P7 P9 P10	0 0 0 0	6 6 6 6	0 0 0 0	1.48 0.65 2.16 3.11	5	5.17 3.33 2.96 2.31	6.840 5.148 4.517 3.702	9.77 9.84 10.00 10.10	20.3	7.25	4.53 5.35 3.84 2.89	-0.090 0.007 0.123 0.159	0.64 0.65 0.67 0.69	58.06 22.41 33.89 16.69	58.70 23.06 34.56 17.38	40.0 22.3 41.0 18.9	0.441 0.434 1.036 0.711

TABLE 1 (Continued)

Run Number	Gage Number	β deg	τ deg	α deg	ξ deg	V_h knots	V_v fps	V_n fps	V_t fps	L_w ft	h in.	θ deg	y percent L_w	P_p psi	P_i psi	P_t , psi		k
																Calc	Exp	
64	P5	0	6	0	1.66	10	0.00	3.415	12.22	30.0	16.0 *	7.66	-0.047	-1.01	15.71	14.70	4.0	0.177
	P7				2.00			3.487	12.20			8.00	0	-1.00	18.91	17.91	12.0	0.509
	P9				1.48			3.377	12.23			7.48	0.058	-1.01	14.21	13.20	9.6	0.434
	P10				1.17			3.311	12.25			7.17	0.073	-1.01	11.87	10.86	10.0	0.470
86	P5	0	0	0	2.74	5	7.02	6.409	12.94	31.2	8.0	-2.74	-0.376	1.13	56.85	57.98	67.5	0.847
	P7				1.79		6.47	6.073	12.82			-1.79	-0.327	1.11	52.48	53.59	89.9	1.256
	P9				0		3.83	3.830	12.62			0	-0.250	1.07	9.11	10.18	6.1	0.214
	P10				0.79		3.83	4.004	12.57			0.79	-0.217	-1.06	14.52	13.46	13.4	0.431
*Correction made for flat crest and trough of the wave.																		

TABLE 2 - COMPARISON OF EXPERIMENTAL AND PREDICTED SLAMMING PRESSURES FOR 10-DEGREE MODEL IN WAVES

Run Number	Gage Number	β deg	τ deg	α deg	ξ deg	V_h knots	V_v fps	V_n fps	V_t fps	L_w ft	h in.	θ deg	y percent L_w	P_p psi	P_j psi	P_t , psi		k
																Calc	Exp	
214	P5, P1	10	6	0	10.65 11.18 12.08	0	4.69	5.182	12.01	29.2	6.29	2.33	0.122	0.33	7.78	8.11	9.58	0.184
	P8, P2						4.36	4.568	12.14			0.98	0.201	0.44	5.60	6.04	7.96	0.197
	P9, P10						3.82	3.646	12.27			-0.82	0.291	0.57	3.04	3.60	3.50	0.136
215	P5, P1	10	6	0	11.05 10.63 10.45	5	7.42	8.571	12.22	29.7	5.90	1.27	-0.180	0.43	20.21	20.64	23.5	0.165
	P8, P2						6.22	7.609	12.10			2.39	-0.102	0.33	16.82	17.15	24.6	0.219
	P9, P10						4.36	5.870	12.12			2.95	-0.022	0.29	10.22	10.51	23.8	0.356
216	P5, P1	10	6	0	11.15 10.69 10.44	10	7.4	9.385	12.41	30.1	6.41	1.05	-0.197	0.46	23.78	24.23	30.0	0.176
	P8, P2						6.1	8.333	12.27			2.20	-0.129	0.36	20.01	20.37	32.0	0.238
	P9, P10						3.92	6.325	12.27			2.99	-0.057	0.29	11.89	12.18	23.9	0.308
217	P5, P1	10	6	0	13.15 11.89 11.03	15	7.64	9.702	12.88	28.9	6.41	-2.59	-0.392	0.72	18.53	19.25	30.3	0.166
	P8, P2						5.66	8.194	12.49			-0.46	-0.272	0.57	15.84	16.41	20.0	0.154
	P9, P10						1.09	4.009	12.34			1.32	-0.185	0.43	4.44	4.87	6.5	0.208
218	P5, P1	10	6	0	12.58 10.76 10.41	15	7.20	9.463	12.89	29.8	6.41	-1.67	-0.336	0.68	19.02	19.70	21.6	0.124
	P8, P2						5.26	8.333	12.33			2.02	-0.143	0.38	19.86	20.24	26.4	0.196
	P9, P10						3.01	6.320	12.29			3.11	-0.043	0.28	11.92	12.20	18.5	0.239
220	P5, P1	10	6	0	13.21 11.10	5	6.70	6.991	12.75	29.7	6.15	-2.67	-0.415	0.71	9.56	10.27	9.1	0.096
	P8, P2						6.30	6.904	12.56			-1.26	-0.316	0.62	10.48	11.10	10.8	0.117
	P9, P10																	
221	P5, P1	10	0	0	10.03 10.01 10.13	0	3.70	3.864	12.57	31.2	5.76	0.75	-0.207	-0.08	4.68	4.60	5.47	0.189
	P8, P2						3.70	3.616	12.65			-0.38	0.272	0.04	4.11	4.15	5.35	0.211
	P9, P10						3.47	3.108	12.72			-1.64	0.351	0.17	2.99	3.16	2.87	0.153
222	P5, P1	10	0	0	10.11 10.01 10.10	10	3.27	3.59	12.27	29.9	6.41	1.49	0.173	-0.15	4.00	3.85	5.0	0.200
	P8, P2						3.60	3.67	12.33			0.32	0.234	-0.03	4.23	4.20	6.2	0.237
	P9, P10						2.84	2.53	12.43			-1.44	0.324	0.15	1.99	2.14	4.4	0.354
223	P5, P1	10	0	0	10.36 10.17 10.01	5	6.75	6.142	12.87	30.9	6.29	-2.74	-0.427	0.29	11.32	11.61	11.8	0.161
	P8, P2						5.89	5.474	12.75			-1.88	-0.356	0.20	9.21	9.41	14.7	0.253
	P9, P10						4.80	4.917	12.52			0.53	-0.222	-0.06	7.59	7.53	14.7	0.313

TABLE 2 (Continued)

Run Number	Gage Number	β deg	τ deg	α deg	ξ deg	V_h knots	V_v fps	V_n fps	V_t fps	L_w ft	h in.	θ deg	y percent L_w	p_p psi	p_i psi	p_t , psi		k
																Calc	Exp	
224	P5, P1 P8, P2 P9, P10	10	0	0	10.04 10.00 10.10	0	8.05 7.20 8.28	7.847 7.264 8.590	12.51 12.34 12.17	30.0	5.76	-0.94 0.30 1.45	-0.303 -0.234 -0.166	0.10 -0.03 -0.14	19.25 16.58 22.89	19.35	24.2	0.203
																16.55	25.2	0.246
																22.75	31.0	0.217
225	P5, P1 P8, P2 P9, P10	10	0	0	10.32 10.14 10.01	0	7.85 6.86 5.66	7.28 6.49 5.55	12.80 12.66 12.51	30.4	5.76	-2.57 -1.71 -0.52	-0.429 -0.352 -0.279	0.27 0.18 0.05	16.00 12.98 9.66	16.27	15.6	0.152
																13.16	16.8	0.206
																9.71	13.5	0.226
226	P5, P1 P8, P2 P9, P10	10	0	0	10.33 10.45 10.29	9.87	6.88 6.43 5.13	6.305 5.758 5.659	12.84 12.87 12.31	30.8	6.55	-2.60 -3.03 2.44	-0.599 -0.450 -0.112	0.28 0.32 -0.24	11.98 9.84 9.70	12.26	14.0	0.182
																10.16	13.0	0.202
																9.46	10.0	0.161
228	P1-P10	10	0	0	10.99	5	0	0.988	12.34	30.0	9.24	4.58	0.022	-0.42	0.27	-0.15	0	--
229	P1-P10	10	0	0	11.07	10	0	1.029	12.34	30.0	9.62	4.77	0.021	-0.44	0.29	-0.15	0	--
230	P5, P1 P8, P2 P9, P10	10	6	0	10.13 10.08 10.32	0	0	0.943 1.014 0.746	12.34 12.34 12.32	30.0	9.50	4.37 4.70 3.46	-0.064 0.024 0.120	0.16 0.13 0.25	0.28 0.32 0.17	0.44	0	--
																0.45	0	--
																0.42	0	--
231	P5, P1 P8, P2 P9, P10	10	6	0	10.19 10.12 10.42	5	0	1.762 1.838 1.544	12.38 12.37 12.41	30.0	8.96	4.08 4.43 3.07	-0.07 0.025 0.130	0.19 0.16 0.29	0.95 1.05 0.71	1.15	2.4	--
																1.21	3.7	--
																1.00	4.8	--
232	P5, P1 P8, P2 P9, P10	10	6	0	10.20 10.14 10.46	10	0	2.62 2.70 2.40	12.41 12.40 12.46	30.0	8.77	3.97 4.33 2.92	-0.070 0.026 0.134	0.21 0.17 0.31	2.10 2.25 1.70	2.31	5.2	--
																2.42	6.4	--
																2.01	4.4	--
233	P5, P1 P8, P2 P9, P10	10	6	0	10.20 10.14 10.46	15	0	3.50 3.58 3.28	12.44 12.14 12.51	30.0	8.77	3.97 4.33 2.92	-0.070 0.026 0.134	0.21 0.17 0.31	3.76 3.96 3.18	3.97	5.3	--
																4.13	8.4	--
																3.49	10.9	--

TABLE 3 - COMPARISON OF EXPERIMENTAL AND PREDICTED SLAMMING PRESSURES FOR VARYING-DEADRISE ANGLE MODEL IN WAVES

Run Number	Gage Number	β deg	τ deg	α deg	ξ deg	V_h knots	V_v fps	V_n fps	V_t fps	L_w ft	h in.	θ deg	y percent L_w	P_p psi	P_i psi	P_t , psi		k
																Calc	Exp	
135	P5, P1	0	6	0* 0.76*	1.42 2.17	5	0	1.874 1.984	12.38 12.40	30.1	10.4	4.59	-0.077	1.03 1.04	4.24 6.57	5.28 7.61	4.5	0.660 0.589
	P7, P2	10	6	1.52*	2.93			2.094	12.42			5.14	0.022	1.04	5.67	6.71		0.529
	P9, P10	20	6	1.52 1.52	10.27 20.36			2.214 1.881	12.40 12.45			3.60	0.1278	0.24 0.19	1.49 0.35	1.73 0.54	3.0 0	0.315 --
136	P5, P1	0	6	0* 0.76*	1.42 2.17	10	0	2.756 2.977	12.40 12.44	30.1	10.4	4.59	-0.077	1.04 1.04	9.18 14.80	10.22 15.84	8.5	0.577 0.494
	P7, P2	10	6	1.52*	2.93			3.197	12.47			5.14	0.022	1.05	13.22	14.27		0.429
	P9, P10	20	6	1.52 1.52	10.27 20.36			3.317 2.983	12.44 12.53			3.60	0.128	0.24 0.20	3.34 0.87	3.58 1.07	6.0 0	0.281 --
138	P5, P1	0	0	0* 0.76*	5.18 4.43	10	0	1.120 1.343	12.35 12.33	30.1	10.4	5.18	0	-1.02 -1.02	0.88 1.50	-0.14 0.48	0	--
	P7, P2	10	0	1.52*	3.67			1.566	12.32			5.15	0.019	-1.02	2.51	1.49		--
	P9, P10	20	0	1.52 1.52	10.63 20.29			1.558 1.535	12.32 12.32			5.04	0.038	-0.35 -0.17	0.71 0.23	0.36 0.06	1.3 0	--
139	P5, P1	0	0	0* 0.76*	5.08 4.33	15	0	1.099 1.433	12.35 12.33	30.1	10.2	5.08	0	-1.03 -1.02	0.87 1.76	-0.16 0.74	0	--
	P7, P2	10	0	1.52*	3.57			1.767	12.31			5.05	0.019	-1.02	3.29	2.27		--
	P9, P10	20	0	1.52 1.52	10.60 20.27	15	0	1.759 1.735	12.31 12.31			4.93	0.039	-0.34 -0.17	0.90 0.30	0.56 0.13	1.7 0	--
140	P5, P1	0	0	0* 0.76*	0.79 1.55	0	6.60	6.428	12.45	29.9	8.24	-0.79	-0.281	1.04 1.04	37.44 53.03	38.48 54.07	34.5	0.430 0.430
	P7, P2	10	0	1.52*	2.31			5.88	12.25			1.03	-0.210	1.04	66.93	67.97		0.430
	P9, P10	20	0	1.52 1.52	10.01 20.02			5.66 6.21	12.09 12.09			2.55	-0.144	0.05 -0.05	10.86 3.90	10.91 3.85	16.3 5.5	0.243 0.074
141	P5, P1	0	0	0* 0.76*	2.11 1.45	0	3.81	4.29	12.33	30.5	7.65	2.21	0.150	-1.02 -1.02	30.91 22.61	29.89 21.59	41.2	1.154 1.154
	P7, P2	10	0	1.52*	0.70			3.97	12.43			0.73	0.219	-1.02	15.91	14.89		1.154
	P9, P10	20	0	1.52 1.52	10.03			7.35	12.43					0.08	4.93	5.02	7.0	0.229

TABLE 3 (Continued)

Run Number	Gage Number	β deg	τ deg	α deg	ξ deg	V_h knots	V_v fps	V_n fps	V_t fps	L_w ft	θ deg	y percent L_w	P_p psi	P_i psi	P_t psi		k
															Calc	Exp	
142	P5, P1	0	0	0*	0.50	5	7.35	7.24	12.52	30.4	-0.50	-0.272	1.06	41.26	42.32	78.6	0.773
				0.76*	1.26			7.35	12.53				1.06	60.79	61.85		0.750
	P7, P2 P9, P10	10 20	0 0	1.52 1.52	2.01 20.02		5.66 5.89	7.47 6.13 6.64	12.53 12.35 12.19		1.12 2.45	-0.199 -0.129	1.06 0.04 -0.05	87.14 11.80 4.47	88.20 11.84 4.43		0.726 0.185 0.091
143	P5, P1	0	0	0*	0.52	5	3.6	3.71	12.43	30.4	0.52	0.228	-1.04	10.99	9.95	14.95	0.560
	P7, P2	10	0	0.76* 1.52* 1.52	0.23 0.99 10.50			3.83 3.94 3.347	12.43 12.43 12.57				1.04 1.04 0.33	10.15 15.43 3.30	11.19 16.47 3.63		0.525 0.496 0.161
144	P5, P1	0	0	0*	0.70	10	5.92	5.77	12.33	29.4	-0.70	-0.275	1.02	28.90	29.92	33.7	0.522
				0.76*	1.46			5.99	12.33				1.02	44.29	45.31		0.484
	P7, P2 P9, P10	10 20	0 0	1.52* 1.52 1.52	2.22 10.00 20.04		6.46 6.46	6.22 7.16 7.52	12.34 12.12 11.90		1.20 2.90	-0.207 -0.138	1.03 0.03 -0.06	64.73 16.13 5.72	65.76 16.16 5.66		0.449 0.243 0.064
145	P5, P1	0	0	0*	2.89	10	4.57	5.188	12.15	30.1	2.89	-0.113	-1.00	35.37	34.37	50.6	0.969
				0.76*	2.13			5.412	12.15				-0.99	47.98	46.99		0.890
	P7, P2 P9, P10	10 20	0 0	1.52* 1.52 1.52	1.37 10.21 20.12		5.90 5.90	5.635 7.111 7.158	12.14 11.99 11.96		3.59 3.81	-0.055 0	-0.99 -0.19 -0.11	37.58 15.47 5.14	36.59 15.28 5.03		0.821 0.159 0.071
146	P5, P1	0	6	0*	2.83	0	2.73	3.414	12.29	30.4	3.17	0.098	1.02	15.59	16.61	16.30	0.721
	P7, P2	10	6	0.76* 1.52* 1.52	3.59 4.35 11.58								1.02 1.02 0.52	12.19 9.91 2.56	13.21 10.93 3.08		0.176
147	P5, P1	0	6	0*	7.19	0	3.70	3.442	12.45	30.0	-1.19	-0.697	1.05	5.81	6.86	2.2	0.096
	P7, P2	10	6	0.76* 1.52* 1.52	7.95 8.71 14.52		4.80	4.096	13.24		-3.07	-0.588	1.05 1.05 0.85	5.12 4.52 2.83	6.17 5.57 3.68		0.086
148	P5, P1	0	6	0*	3.88	5	1.85	3.186	12.32	29.8	2.12	0.146	1.02	9.77	10.79	11.0	0.559
				0.76*	4.64			3.296	12.34				1.03	8.62	9.65		0.522
	P2	10	6	1.52* 1.52	5.40 12.84		2.51	3.405 3.476	12.36 12.52		-0.59	0.277	1.03 0.66	7.82 2.48	8.85 3.14		0.489 0.120

TABLE 3 (Continued)

Run Number	Gage Number	β deg	τ deg	α deg	ξ deg	V_h knots	V_v fps	V_n fps	V_t fps	L_w ft	h in.	θ deg	y percent L_w	P_p psi	P_i psi	P_t , psi		k
																Calc	Exp	
149	P5, P1	0	6	0*	8.66	5	3.92	4.220	12.56	29.4	8.17	-2.66	-0.640	1.06	6.85	7.91	3.7	0.107
	P7, P2	10	6	0.76* 0.52* 1.52	9.42 10.17 15.03		4.328 4.435 4.969	12.59 12.62 12.75				-3.76	-0.571	1.06 1.07 0.81	6.40 6.05 3.94	7.46 7.12 4.75		0.102 0.097 0.075
150	P5, P1	0	6	0*	8.55	0	5.79	5.215	13.02	29.0	7.26	-2.553	-0.37	1.14	10.63	11.77	13.2	0.250
	P7, P2	10	6	0.76* 1.52* 1.52	9.31 10.07 12.90		5.208 5.535	13.09 13.16 12.24				-0.68	-0.279	1.15 1.17 0.63	9.42 8.45 6.23	10.57 9.62 6.86		0.250 0.251 0.136
151A	P7, P2	10	6	1.52	14.91	5	3.70	3.995	12.84	30.2	7.65	-3.61	-0.551	0.82	2.58	3.40	2.80	0.090
152	P5, P1	0	6	0*	3.95	10	5.66	7.861	12.27	29.9	8.6	2.06	-0.171	1.01	58.41	59.42	34.4	0.287
	P7, P2	10	6	0.76* 1.52* 1.52	4.70 5.46 10.66		8.080 8.299 4.26	12.31 12.36 12.19				3.80	-0.079	1.02 1.03 0.35	51.01 45.84 15.30	52.03 46.87 15.65		0.272 0.257 0.211
153	P5, P1	0	6	0*	6.25	15	4.00	6.577	12.81	30.6	7.86	-0.254	-0.740	1.11	24.88	25.99	25.3	0.301
	P7, P2	10	6	0.76* 1.52* 1.52	7.01 7.77 13.67		6.904 7.228 2.26	12.88 12.97 13.11				-1.86	-0.33	1.12 1.13 0.79	24.07 23.24 4.86	25.19 24.37 5.65		0.274 0.250 0.098
154	P5, P1	0	6	0*	6.63	10	3.82	5.440	12.48	29.3	7.65	-0.63	-0.725	1.05	15.96	17.01	19.1	0.333
	P7, P2	10	6	0.76* 1.52* 1.52	7.38 8.14 13.76		5.657 5.873 2.40	12.53 12.59 12.67				-1.99	-0.335	1.06 1.07 0.74	15.19 14.43 3.16	16.24 15.50 3.90		0.308 0.285 0.173
*Assumed value																		

INITIAL DISTRIBUTION

Copies

1 CNO
1 NOP 098T

3 CHONR
1 ONR 438
1 ONR 439
1 ONR 463

1 CHONR, London

1 NRL

1 NAVMAT
1 Mat 0341

1 USNA

1 USNAVPGSCHOL

6 NAVSHIPSYSKOM
1 SHIPS 031
1 SHIPS 034
2 SHIPS 2052
1 PMS 391
1 PMS 395-A2 (S. Lum)

3 NAVAIRSYSKOM
1 Aero & Hydro Br (Code 5301)
1 Struc Br (Code 5302)
1 Engr Div (Code 520)

2 NAVFACENGCOM
1 FAC 03
1 FAC 04

1 NAVORDSYSKOM
1 ORD 03

1 NOL

1 NAVSHIPYD BSN

1 NAVSHIPYD BREM

1 NAVSHIPYD CHASN

1 NAVSHIPYD LBEACH

1 NAVSHIPYD NORVA

1 NAVSHIPYD PEARL

1 NAVSHIPYD PTSMH

1 NAVSHIPYD SFRANBAY VJO

Copies

7 NAVSEC
1 SEC 6110
1 SEC 6113
1 SEC 6114
1 SEC 6114F
1 SEC 6128
1 SEC 6132
1 SEC 6136

12 DDC

2 Coast Gd.
1 Chief Testing & Development Div
1 Ship Structures Committee

1 Lib of Congress

1 MARAD

1 NAS

1 Nat'l Sci Foundation

2 Catholic Univ
1 Prof M.C. Soteriades
1 Prof S.R. Heller, Jr.

1 Univ of Calif

1 St. Univ of Iowa

1 MIT, Attn: Dr. A.H. Keil

2 Univ of Michigan
1 Prof H. Benford
1 Prof F.T. Ogilvie

1 SWRI, Attn: Dr. C.R. Gerlach

1 SIT

2 SNAME
1 Slamming Panel

1 American Bureau of Shipping

1 Oceanics, Inc., Attn: Dr. P. Kaplan

1 Poseidon Sci Corp
Attn: Mr. W. Marks

CENTER DISTRIBUTION

Copies	Code
1	15
1	152
1	154
1	156
1	16
1	17
1	172
1	173
1	178
25	9424

UNCLASSIFIED

Security Classification

DOCUMENT CONTROL DATA - R & D

(Security classification of title, body of abstract and indexing annotation must be entered when the overall report is classified)

1. ORIGINATING ACTIVITY (Corporate author) Naval Ship Research and Development Center Bethesda, Maryland 20034		2a. REPORT SECURITY CLASSIFICATION UNCLASSIFIED	
		2b. GROUP	
3. REPORT TITLE SLAMMING TESTS OF THREE-DIMENSIONAL MODELS IN CALM WATER AND WAVES			
4. DESCRIPTIVE NOTES (Type of report and inclusive dates) Final			
5. AUTHOR(S) (First name, middle initial, last name) Sheng-Lun Chuang			
6. REPORT DATE September 1973		7a. TOTAL NO. OF PAGES 57	7b. NO. OF REFS 8
8a. CONTRACT OR GRANT NO. b. PROJECT NO. c. In-House Work Unit 4-1700-001 d.		9a. ORIGINATOR'S REPORT NUMBER(S) 4095 9b. OTHER REPORT NO(S) (Any other numbers that may be assigned this report)	
10. DISTRIBUTION STATEMENT APPROVED FOR PUBLIC RELEASE: DISTRIBUTION UNLIMITED			
11. SUPPLEMENTARY NOTES		12. SPONSORING MILITARY ACTIVITY Surface Effect Ships Program Office (PM 17)	
13. ABSTRACT <p>A prediction method is being developed at the Naval Ship Research and Development Center (NSRDC) for determining wave impact loads when a high-performance vehicle experiences slamming while traveling at very high speeds. This method is based on the Wagner wedge impact theory, the Chuang cone impact theory, and NSRDC drop tests of wedges and cones. Determination of impact velocity is based on the hypothesis that it is equal to the relative velocity between the impact surface of the moving body and the wave surface. As part of the development of this prediction method, slamming tests of three-dimensional models were conducted in calm water and waves, and the results were recorded during the time of impact when the model traveled with both horizontal and vertical velocities. The agreement between experimental and predicted results was remarkably good. The effect of elasticity on slamming was also investigated during the tests. As expected, results clearly indicated a reduction in impact pressure due to elasticity effect.</p>			

UNCLASSIFIED

Security Classification

14. KEY WORDS	LINK A		LINK B		LINK C	
	ROLE	WT	ROLE	WT	ROLE	WT
Slamming Ship Slamming in Waves Structural Response to Slamming Load Three-Dimensional Slamming Prediction of Three-Dimensional Slamming Load Elasticity Effect on Slamming Load						